2-7-2011

Off-peak summer performance enhancement for rows of fixed solar thermal collectors using reflective surfaces

Casiano Armenta

Follow this and additional works at: https://digitalrepository.unm.edu/me_etds
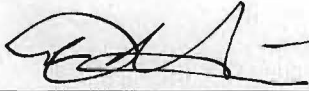
Casiano C. Armenta
Candidate

Mechanical Engineering
Department

This thesis is approved, and it is acceptable in quality
and form for publication:
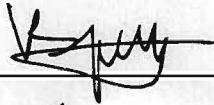
Approved by the Thesis Committee:
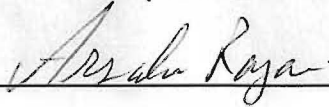
Andrea Mammoli   , Chairperson

Peter Vorobieff

Arsalan Razani

**OFF-PEAK SUMMER PERFORMANCE ENHANCEMENT
FOR ROWS OF FIXED SOLAR THERMAL COLLECTORS
USING REFLECTIVE SURFACES**

BY

CASIANO CROWLEY ARMENTA

**B.S., ENGINEERING TECHNOLOGY, NEW MEXICO STATE
UNIVERSITY, 2000**

THESIS

Submitted in Partial Fulfillment of the
Requirements for the Degree of

**Master of Science
Mechanical Engineering**

The University of New Mexico
Albuquerque, New Mexico

December, 2010

Dedication

To my grandparents, Jesus & Carmen Armenta and David & Elsie Crowley

Acknowledgments

I would like to thank my parents, Randolfo & Barbara Armenta, who have always been there for me and for providing their help and support throughout my entire life. I would also like to thank my advisor, Professor Andrea Mammoli, for giving me the opportunity to work on this project and to my other committee members, Professor Peter Vorobieff and Professor Arsalan Razani, for their time and guidance throughout this thesis. There are also many thanks to the graduate students under Professor Mammoli and employees of the Mechanical Engineering Department for their help and support, especially Stoney Haver for helping install countless mirrors on the roof. Lastly, I would like to give a very special thank you to my wife, Angelica Armenta, for her love and support over the years, and for whom this thesis would not be possible.

**OFF-PEAK SUMMER PERFORMANCE ENHANCEMENT
FOR ROWS OF FIXED SOLAR THERMAL COLLECTORS
USING REFLECTIVE SURFACES**

BY

CASIANO CROWLEY ARMENTA

ABSTRACT OF THESIS

Submitted in Partial Fulfillment of the
Requirements for the Degree of

**Master of Science
Mechanical Engineering**

The University of New Mexico
Albuquerque, New Mexico

December, 2010

Off-Peak Summer Performance Enhancement for Rows of Fixed Solar Thermal Collectors using Reflective Surfaces

by

Casiano Crowley Armenta

B.S., Engineering Technology, New Mexico State University, 2000

M.S., Mechanical Engineering, University of New Mexico, 2010

Abstract

The possibility of increasing the efficiency of fixed solar thermal collectors without greatly adding to the cost or complexity of the overall solar collection system was studied. The focus was on the use of flat mirrors, which would accomplish this goal by capturing the morning sunlight during the summer non-peak solar collection time while maintaining the balance of the system within its existing design specifications, allowing the system to perform at a higher capacity factor. A 150kW$_t$ solar heating and cooling system operates within the Mechanical Engineering Building at the University of New Mexico and was the basis for a simulation model and validation testing. The use of flat mirrors to increase solar energy collection is a cheaper alternative to the purchase of additional solar collectors and results show that the reflectors, properly installed on a solar thermal collection system, can reduce the cost of cooling by 20% without further modification to the existing system.

Contents

Contents

List of Figures

List of Figures

List of Tables

Glossary

$ United States Dollar

Absorption Chiller   A machine using solar hot water and cooling tower water to generate chilled water

CWT   Chilled Water Tank

ft   Feet

Gray Surface   Has radiation properties that are independent of wavelength, its surface is diffuse, and the incident energy over the surface is uniform [8]

Histogram   A graphic depiction of the quanitity of pixels at different levels of the gray scale

HWT   Hot Water Tank

HVAC   Heating, Ventilation and Air-Conditioning

IAM   Incidence angle modifier

Lennox LSC-18   A solar flat-plate collector

Licor LI-200   A brand of pyranometer

Glossary

ME	Mechanical Engineering
m	Meters
MDT	Mountain Daylight Saving Time in the United States
MST	Mountain Standard Time in the United States
Payback	The initial cost divided by the uniform annual benefit [9]
Physical Plant	A power plant on the UNM main campus
Pyranometer	An instrument used to measure solar flux
ReflecTech®	A reflective material that is made by a company named ReflecTech®
Reflectivity	The fraction of incoming radiation which is reflected from a surface
Solar Flux	The sun's radiational energy over a given area (W/m^2)
Solar Noon	The time the sun crosses the meridian of the observer [8]
Solar Time	Time based on the apparent angular motion of the sun across the sky [8]
Sunda Seido 1-16	A solar vacuum tube collector
TOU	Time-Of-Use
UNM	University of New Mexico

Chapter 1

Introduction

1.1   Overview

In the late 1970's, the United States was experiencing increasing oil prices which drove higher consumer costs in gasoline and heating oil. In response, the scientific community began searching for an efficient alternative source of energy that would reduce the country's dependency on oil. During this time, the University of New Mexico (UNM) was designing a new building for the Mechanical Engineering Department. Given the poor state of the economy at that time, and the public interest in alternative energy sources, UNM decided to take advantage of their situation by working with the building's designers to establish a solar assisted thermal storage system that would not only reduce the cost necessary to run the heating, ventilation and air-conditioning (HVAC) system, but also provide a system upon which the university could begin to conduct research in the field of renewable energy. Albuquerque, New Mexico was an ideal location for this research because it averages 278 non-cloudy days per year [10].

The design of the system was eventually included eight 14,000 gallon tanks of

thermal storage, kept in the basement, that would heat the building in the winter and cool it in the summer. In the winter, hot water created by solar energy, combined with a heat pump located within the building and auxiliary steam from the UNM Physical Plant, was used to heat the complex. An air to air heat recovery system was also installed to reduce the amount of heat lost when fresh air was supplied to the building. Solar energy collected during the warmer seasons was used to power an organic Rankine cycle turbine to generate electricity that was fed into the electrical grid. A chiller powered by electricity would run at night, cooling the water in the tanks. By running the chiller during evening, off-peak hours the cost of electricity was cut by almost 50% [11]. The new building opened in the 1980-1981 academic year and the price of oil had peaked to over \$33.77 a barrel [12]. The price of oil would later drop dramatically to \$12.51 in 1986 [12], signaling the beginning of the end for UNM's fledgling project. As a result of the price drop in oil, the demand for cheaper energy sources vanished from the public mind and funding to support the continuation of renewable energy research also disappeared. At a time when issues with the thermal storage system were being discovered and needed repairs were being identified, the lack of interest and funding forced the project and system to be abandoned.

Fast forward to the mid 2000's where history seems to repeat itself, with one important exception. Not only were the prices of oil increasing, there was a spreading political awareness of the risks posed to the United States by its dependence on foreign oil. These realities renewed public interest in alternative energy sources. As a result, the Mechanical Engineering Building's solar and thermal storage system was refurbished and modernized. The upgraded system was designed to use the solar energy collected during the summer months, not to generate electricity as had been done with the original system, but to feed into an absorption chiller that in turn assists in cooling the building. Hot water generated by the solar collectors was now stored in a single tank that fed the absorption chiller, and up to seven tanks

of chilled water could be used to cool the building. The hot water storage tank was itself updated with better insulation that allowed for a reduction in the volume of the tank from 14,000 gallons to 9,000 gallons. The new solar absorption cooling system is capable of producing enough chilled water to charge the equivalent of one tank each day. The other tanks continue to be replenished with chilled water generated by electric chillers operated during evening, off-peak hours, by the UNM Physical Plant. During the winter, only one storage tank is utilized to heat the building, with most of the energy from the solar collectors being used directly.

When the HVAC system is running at its optimal performance, there is almost enough solar energy produced, approximately 90%, to heat the building during the winter. The solar energy collected in the summer can only provide approximately 40% of the energy needed to cool the building. Much of the equipment associated with the solar collection system (e.g. chiller, pumps) is underutilized for a large fraction of each day, giving rise to the possibility of producing more chilled water to lessen the cost of electricity for cooling. One option would be to install additional solar collectors on the roof. Unfortunately, this requires increased space to add more rows with sufficient spacing between them to prevent shading on a roof that, in the case of the UNM building, is already almost completely covered in solar collectors. In addition, more piping and larger pumps would be needed to support the higher volume of water that would be circulated when the maximum designed energy load of the system is surpassed.

A second option is to install tracking mirrors that would follow the sun throughout the course of the day, reflecting the sun's radiation onto the collectors for a longer period. This could increase the solar collection by two or three times during any given time of day. Although the cost of the mirrors would be less than the cost of installing new solar collectors, once combined with the purchase and installation of a tracking system (i.e. motors, gears, electronics, etc.), larger pumps to support the

higher volume of water being circulated, and the likely maintenance costs associated with the use of mechanical devices in the elements common to the region (wind, sand, ice, snow), the total cost of this option could also be great.

A major problem with the above options is that they both increase the solar collection of the system to the point of surpassing the current maximum design load of the pump flow rates, driving an increase to the cost of the system by having to compensate with larger pumps. It is clear that this problem must be addressed if we want to develop a solution with a reasonable cost. The amount of solar flux recorded throughout the day is measured in watts per square meter (W/m^2). When plotted, it forms the shape similar to a sine curve (from 0 to π) on a sunny day (Figure 1.1). The peak of the curve is the maximum load considered when designing the system. Modifying the shape of the curve so that the peak flux extends for a substantial fraction of the day, where the plateau occurs at the maximum load design of the system, means there would be no need to update the pumps of the existing system. Achieving a plateau at the system's maximum load is achievable by ramping up the solar collection in the morning and allowing it to drop off during peak conditions. This concept would increase the amount of solar energy collected, but not strain the entire system as was the case with the previous options.

As a result of these considerations, the last option, which is the basis of this thesis, involves the implementation of stationary, flat mirrors to achieve the plateau effect of solar flux hitting the solar thermal collectors during the morning solar radiation, a decision which is explained further in this paper.

It is important to note the location of the peak in Figure 1.1 which is just before 1400 hours Mountain Daylight Saving Time (MDT). In the United States, conversion to daylight savings time during the summer is typical. Solar time in Albuquerque, NM is within plus or minus one half hour of the Mountain Standard Time (MST) and MDT is one hour ahead of MST. Therefore, solar noon occurs at plus or minus
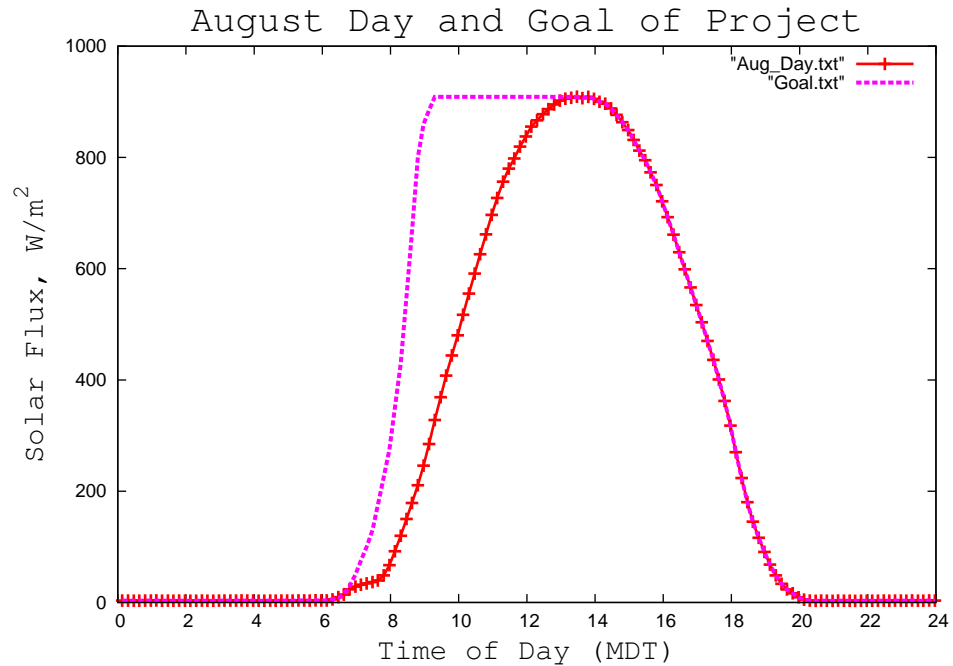
Figure 1.1: A graph showing solar flux measurements collected on a clear sunny August day in Albuquerque and a projected goal of increased solar flux striking the surface of the solar collectors.

a half hour of 1300 hours. The orientation of the Mechanical Engineering Building is not facing due south. It is facing 13° West of South, which explains the location of the peak in the above graph and the graphs throughout this paper.

1.2   Literature Review

Before determining the final design of this system's installation, a review of the research accomplished in the past on the topic was conducted. This topic has been studied for many years and covers a wide range of positions and locations relative to the installation of flat plate reflectors and solar collectors. The use of simulation and modeling, at times in conjunction with prototype testing, were the common methods

practiced from the late 1950's to the present day.

In 1958, Tabor [13] believed that "a completely fixed mirror cannot provide any useful concentration." The only way to get any useful concentration was thought to be the use of a cylindrical mirror in a parabolic shape whose axis was in the East West direction, the same direction as the collector. The mirror would need to be adjusted weekly, but could provide a concentration increase by a factor of 3. In addition, he concluded that adding a second stage concentration could provide a concentration increase by a factor of 4.

By the mid 1960's, Tabor [14] changed his way of thinking as evidenced by a conference paper in which several different methods on the use of a flat reflector on a flat collector were discussed and tested by simulation. One method was to install a mirror above and/or below the collector. The angle of the reflectors would be approximately 120 degrees or less from the surface of the collector. The goal of these reflectors was to make sure the solar noon reflection was hitting the collector. The disadvantage to this methodology was that the reflector needed to be adjusted weekly. The reflector above the collector would be needed for the winter months and the reflector below the collector would be needed for the summer months. Another method discussed was the installation of reflectors on the East and/or West side of the collector. When only using one reflector, a 90° or greater angled mirror to the collector would be installed on the West side during the morning and rotated by a hinge to the East side of the collector during the afternoon. This would provide reflection throughout the day, except for solar noon. A reflector could also be installed above or below the collector depending on the season. The last method discussed involved placing reflectors on all sides of the collector. These mirrors would be adjusted throughout the day to track the sun. It was discovered that regardless of the mirror configuration, the reflectors could increase the energy collected by a factor of approximately 2. When using reflectors above or below the collector, the energy

gained could product a very large peak at solar noon, while placing the reflectors on the East and West sides of the collectors tended to provide a more uniform energy collection.

During this same period, Souka and Safwat [15] were studying the use of a double-exposure, flat-plate collector paired with a three piece reflector by mathematical simulation. They faced the collector south and placed the three piece reflector behind it so that the collector received solar energy in two ways, directly from the sun on the front and reflected solar energy from the back. The three piece reflector was designed like a tri-fold. The center reflector faced the back of the collector directly and the side reflectors were angled so that the solar energy hitting them would be directed toward the back of the collector. This study was preformed for a location of 30° North latitude. The optimum angles of the collector and reflectors on the first day of each month between 9 am and 3 pm were determined by deriving equations.

At the University of New Mexico in 1966, Merchant and Cobble [16] used a square collector that was placed horizontal to the ground and had a reflector attached to either side. The width of each of the four reflectors was the same as the collector, but with a length that was considerably longer. The reflectors were 0.51 feet wide, identical to the collector, but at a length of 5 feet, and adjustable. The maximum energy collected occurred when the angle of the reflectors was at approximately 6 degrees from vertical. That was proven both theoretically and experimentally.

By 1968, Souka and Safwat [17] had developed another theoretical approach using the same double-exposure, flat-plate collector design, this time pairing it with a single reflector. The collector was exposed to direct sunlight on one side and reflected sunlight on the other side. Derived equations, based on energy incident upon the collector and the heat transfer of the collector, were used on a 30° North latitude on May 1 under certain conditions. A graphic representation of the equations illustrated that peak performance of energy absorbed from 9am to 3pm was increased with the

7

reflector.

In the early 1970's, the quality of the reflectors being used with the solar collection systems began to be the focus of new studies. Thomason and Thomason [18] began recording their observations of a residential scale system in which aluminum reflectors were used at the bottom of the collector. When the reflector was installed, it had a reflectivity of 70%, but after 10 years the reflectivity dropped to 30%. A coat of aluminum paint was applied to improve the quality, but the reflectivity diminished faster than with the original reflector.

Studies into the positioning of reflectors and solar collectors also continued. A solar house built in Coos Bay, OR was the basis of a 1975 study by D.K. McDaniels *et al.* [19]. In this study, a solar home was built with collectors positioned almost vertical and aided by a reflector. The results of the study showed that when the reflector was positioned perpendicular to the collector, it provided the optimum angle for collecting energy. The collectors were positioned for increased winter collection, but the study showed that the same principle could be applied for collection during any season.

In 1975 at the University of Colorado, Seitel [20] used a FORTRAN code to find the optimum setup for a flat-plate collector that was horizontal to the ground and used a reflector on one side of the collector. Different sizes, shapes and orientations of both the collector and reflector were run through the program. It was again proven that a reflector could provide a great improvement to the collector's ability to gather energy, especially when the collector is forced into non-ideal positions such as the architecture or direction of a building. The optimum position for the reflector/collector system should be in the East-West direction with the reflector on the North side of the collector.

Another mathematical simulation was preformed in 1976 by Grassie and Sheri-

dan [21], to simulate a reflector above and then below the collector of a hot water system. The results revealed three primary considerations that are key to designing an adequate reflector/collector system: the system should be created to meet the required energy load under the weather conditions for that region, the effects on performance of diffuse energy from the reflectors to the collector is very little, and reflectors can increase the energy collected by the system, but is only advantageous depending on the cost of the reflectors and collectors.

Additional simulations were preformed by Baker *et al.* [22] at the University of Oregon using a FORTRAN code to simulate the effects of a reflector on a solar collector over the course of an entire day. The angle at which the maximum enhancement of collection occurred was calculated to be between 90° and 95° between the reflector and collector, when the reflector length was unlimited. If the ratio of reflector to collector length was 2 to 1, then the optimum angle changed to 100°.

In 1978, Espy [23] studied the advantages of one or two reflectors either above or below the collector to increase either winter or summer energy collections. This work indicated that an increase of 50% to 175% could be obtained when the system was set up for year round collection. When set up for seasonal collection, an increase of 60% to 200% could be obtained. The percentage increase depended on the amount of adjustments that were made throughout the year or the season. The cost of the materials needed for this enhancement ranged from 5% to 30% of the cost of the solar collectors themselves.

During the same period, Los Alamos researchers Grimmer *et al.* [24] were doing a study based on a previous journal article, in which a vertical collector was used for gathering energy for the winter with the aid of a reflector that was horizontal to the ground. The authors wanted to find the direct and diffuse energy that was reflected off different surfaces. The surfaces used in this experiment were a mirror, a sheet of aluminum, a sheet of plywood coated in white paint, and a sheet of plywood coated

in silver paint. The results of the mirror and the aluminum sheet were found to be very similar with a total reflectivity of approximately 0.82. The reflectivity of the silver painted surface tested at 0.516, but if the surface were smooth, the reflectivity could be 0.728. The white painted surface provided the poorest reflectivity. In fact, it was found that the collector's performance was better if it was oriented at the angle of 55° without the aid of the reflector, than if the collector were vertical to the ground with the a horizontal white painted reflector.

At the University of Houston, Mannan and Bannerot [25] were studying the effects of a trough system with infinite length in the East-West direction using one or two mirrors on the North and South side of the collector by simulation. The collector was positioned flat on the ground with only adjustments made to the angle of the mirrors. The maximum energy collected occurred when the acceptance angle was at 9°, meaning that the angle of the sun's rays were 9° from vertical. At this angle, one mirror on each side could produce a concentration ratio of 2. Installing two mirrors on each side could produce a concentration ratio of 2.6. These concentration ratios were calculated when the reflectivity of the mirrors was at 100%. The disadvantage was that the mirrors required many adjustments throughout the year.

Bannerot and Howell [26], at the University of Houston, studied the effects of a reflector above and below the collector to find the increase in daily and yearly average radiation performance using both simulation and experimentation. The width of the reflector to collector ratios ranged from 1.1:1 to 5:1. The systems with no adjustments provided little improvement in the energy collected. For those systems that were adjusted semiannually or monthly, the increase in energy collected could be 2 or 3 fold.

In 1979, at Drexel University, Larson [27] explored the theoretical idea of a reflector on the front side of the collector along with a reflector on the back side of the collector. The rear reflectors were evaluated with both stationary and adjustable

mirror configurations. The collector was installed in the vertical position. The latitude locations for this study were 35°, 40° and 45°. There were three rear reflectors. The first reflector was placed on the ground, perpendicular to the collector. The second reflector was connected to the first reflector, but at a much steeper angle. The third reflector was connected to the second reflector, but is near vertical. The angle of the third reflector from vertical was the same angle that the front reflector was from horizontal. The reflectivity of the mirror was assumed to be 0.88. During the winter months, the stationary system demonstrated an average enhancement factor of 1.85, whereas the adjustable system had a factor of 2.25. It was discovered that adjustable reflectors provided better results for both winter and summer.

Larson [28] later studied by simulation the optimum placement of a single reflector on a collector. The focus was on using a reflector, with assumed reflectivity of 0.88, below the collector. For a year-round, stationary collection system, the collectors should be set up at an angle of 15° greater than the latitude of the location for optimal collection. For a reflector with an equal length to the collector, the reflector should be at 55° minus the latitude of the location for its optimal performance. For a reflector that is two times the length of the collector, the reflector should be set at 65° minus the latitude of the location to maximize its performance. The energy collected was increased when the system was adjusted semi-annually or more during the year.

In 1980, Rudloff *et al.* [29] performed studies on a collector that was placed at an angle between 50° to 90° with a reflector attached to the bottom. The reflector had the same area as the collector and a reflectivity of 0.82 was assumed. The analysis was conducted for Salt Lake City, UT. When the reflector was placed at an angle of 5° to 10° above horizontal and the collector was placed close to vertical, the optimum performance could be found. There was a 16% and a 28% increase of yearly output per unit collector area for domestic hot water and space heating, respectively.

Chapter 1. Introduction

Research was also being conducted by Taha and Eldighidy [30] to find out how collectors that are not facing due South could be more effective with the use of reflectors. This study addressed the fact that many buildings were not built facing due south, which is the ideal position for solar collectors. The modeled reflectivity of the reflectors was assumed to be 0.8. The results were that the reflectors could increase the energy collected up to 13.1 percent, but the reflectors needed to be adjusted at least once during the year. This study determined that in order for the solution to be cost effective, the cost of the reflectors should be kept to about 10 percent of that of the collectors. In addition, the reflectors should only be used for collectors that are off-South by 22 degrees or less for whole year operations in order to keep the enhancement benefits greater than the overall cost.

By 1981, Chiam [31] wanted to understand the advantages and disadvantages of either one reflector (above or below the collector) or two reflectors (above and below the collector), and conducted his research by simulation. It was discovered that the higher the reflector/collector width ratio, the better the performance. Two key factors the study identified for consideration when designing a system was the angle of the collector and the tilt of the reflectors with respect to the collector. It was found that one reflector on a collector increases the performance, but two reflectors provided better results. What limited the reflector's effectiveness was that they only provided increased performance during a season and not for the entire year. The reflectors needed to be adjusted seasonally for better energy collection.

In 1982 Chiam [32] conducted a simulation-based study to determine whether a reflector installed on the top of a collector or at the bottom would provide the greatest increase in energy collected during the winter months. If the collector was installed at the latitude angle, the reflector needed to be above the collector for best performance. If the collector was installed at a more vertical angle for better winter collection, then the reflector needed to be below the collector for best performance.

12

If the angle of the collector was less than the latitude angle, better for summer collection, the reflector worked best if installed above the collector. The latter was not found to be as efficent as the previous two methods when the goal was to obtain a higher collection during the winter months.

Chiam [33] also studied by simulation ways to increase the performance of V-trough concentrators while making minimal adjustments throughout the year. When the collector was tilted at the latitude angle and the reflector width was 1.5 larger than the collector, the solar beam enhancement could reach 1.6. Adjustments were needed at least twice a year, with larger increases in energy coming when more adjustments were made throughout the year.

Another project Chiam [34] developed sought further understanding of the advantages of only one reflector, either above or below the collector, as compared to two reflectors, one above and one below by simulation. This study differed from a previous, similar project in that the lengths of the reflectors had to be longer than the collectors and a reflectivity of 0.8 was assumed. When increasing winter collection with only one reflector, and the collector was at its optimum year round tilt, the reflector was needed above the collector. If the collector was set for winter collection, the reflector was needed below the collector. When increasing the summer collection with only one reflector, then the opposite needed to be preformed. For year round collection, the best method was to install reflectors above and below the collector, also known as a V-Trough Concentrator. The disadvantage found with the V-Trough setup was that it could not provide peak seasonal performance unless adjustments were made for the season.

By 1988, Garg and Hrishikesan [35] were studying the effect of reflector angles with respect to the collectors by a theoretical model. They studied a collector that was set to a zero angle versus one set to the latitude angle of the location. Two reflectors were set above and below the collector and could be adjusted to any angle.

The study was performed for three different locations in India over three different months (March, June, and December). Shading of the reflectors onto the collectors was taken into consideration. The greatest improvement in energy absorption was found when a zero tilt angle collector was aided by reflectors during the month of December. The data from the month of June showed that if the collector was positioned horizontal to the ground, or to the latitude angle, the amount of energy absorbed was about equal.

During the same period, Faiman and Zemel [36] wanted to reduce the overall height of a solar collection system by changing the optimum year round angle of the collector. Reducing the height of the solar collectors was desirable from an architectural perspective. While lowering the angle of the collectors could improve the energy collection during the summer, mirrors were needed to make up for the loss of energy collected in the winter. This study was performed by simulation with a reflector placed above the collector and proved winter enhancement could be achieved.

In 1995, Kaushik *et al.* [37] studied the performance of a collector that was set at different angles to the south and different azimuth angles. Reflectors were installed above and below the collector and were sized with the same length as the collector, but could have different widths. Shading of the reflectors on the collector was accounted for and a reflectivity of 0.8 was assumed for the reflectors in the simulation model. It was found that the peak performance of the collectors could be increased by 44% in the winter and 15% in the summer.

In 2000, Hussein *et al.* [38] studied how a planar collector could be enhanced by using a reflector on the upper edge of the collector. The purpose was to assess the improvement resulting from changing the angle of the reflector beginning once a year to once a day by theoretical analysis. It was found that changing the reflector angle twice a year provided the greatest effect, boosting the yearly energy collection by

approximately 13%. To obtain this increase in yearly collection, the reflector length had be longer on each side of the collector by the width of the collector and the reflector width had to be equal to the collector width.

The above summarizes the recent research that has been accomplished using flat mirrors on solar collectors. It is important to note that the prior research accomplished was conducted with the goal of increasing the peak performance of the solar collector. The aim of the current work is to improve energy collection by increasing the time of operation at peak performance, rather than increasing the peak itself. Moreover, the fact that there are several rows of collectors place much stricter constraints on the location of the reflector then is the case with individual rows of collectors.

1.3 UNM's Solar Collection Heating and Cooling System

The ME building's heating and cooling system is more complex than what is found on buildings of this size. To better understand the entire system, a schematic is provided that illustrates the major components and how future mirrors would work together (see Figure 1.2). The solar collectors, at the top of the drawing near the sun, absorb radiation from the sun and transfer the heat to a mixture of water and glycol, or propylene, which is pumped through the collectors to a heat exchanger in the basement of the building. Water from the bottom of the hot water tank (HWT) is pumped out and piped to the heat exchanger once the temperature of the water/glycol mixture reaches a set point of 94 °C. The pumps adjust the flow rates of the propylene and the water from the HWT to maintain the set point temperature coming out of the collectors. The water/glycol mixture, which has been cooled after

exiting the exchanger, is recirculated to the solar collectors. With the addition of the reflectors to the solar collectors, the set point of the system will be reached sooner and the duration for the peak solar output of the collectors will be extended. This will increase the total amount of hot water stored in the HWT.
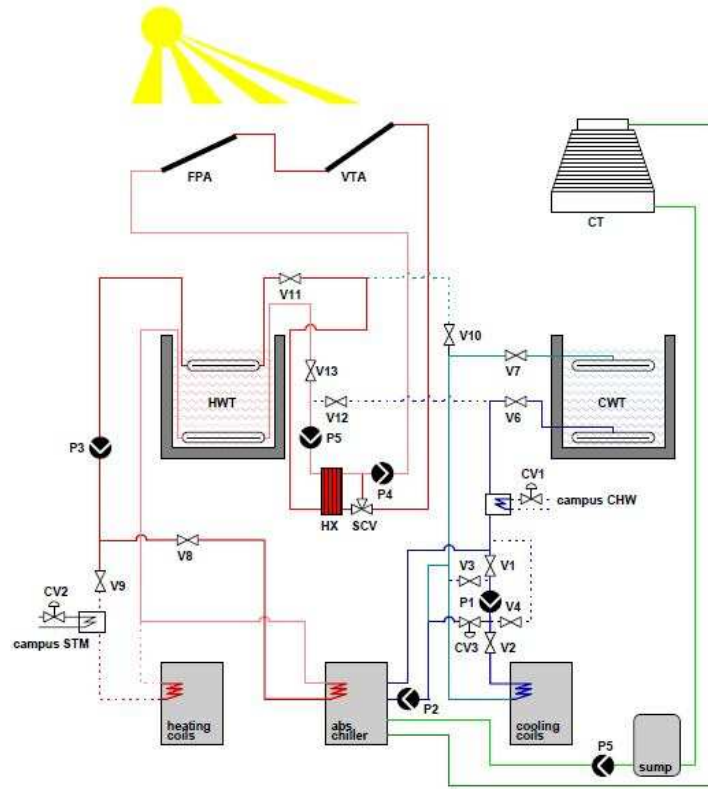
Figure 1.2: Schematics of the UNM ME solar thermal system

Once 11,356 liters (13,000 gallons) at a temperature over 82.2 °C accumulated in the HWT, the tank is ready to supply hot water to the absorption chiller, located at the bottom center of the schematic. The three sets of piping connected to the absorption chiller are the hot water from the HWT, cool water from the cooling tower (CT) and return water from cooling coils which is subsequently tied back upstream of the coils. In the drawing, the campus chilled water system serves the additional cooling needs that cannot be provided by the absorption chiller, by charging the

chilled water (CHW) tanks at night

The process of generating heat for a building is very simple. Water from the HWT goes to a heating coil and a fan blows air over the heat exchanger to provide heat for the building. There is a campus steam (STM) supply for when the solar collection system alone cannot provide enough heating, similar to the CHW described for the cooling process. A heat exchanger boosts the water temperature before it reaches the heating coils if the temperature is below set point.

1.4   Absorption Chiller

An absorption chiller is used to produce cold water that cools the Mechanical Engineering building. The absorption chiller requires three types of inputs to generate chilled water at approximately $7\,°C$. The first is return chilled water from the cooling coils that is at approximately $20\,°C$. The second is cool water from a cooling tower, and the last is solar hot water from the HWT that must be above $70\,°C$. The absorption chiller is made up of two chambers, one of which is under vacuum. In the vacuum chamber, water (the refrigerant) drips on the outside of a heat exchanger, removing heat from the return chilled water within it. Lithium bromide liquid is contained at the bottom of the vacuum chamber to absorb the water vapor in the tank, keeping the chamber under vacuum. As the lithium bromide becomes saturated with water vapor, its capacity to absorb is reduced. To solve this problem, the lithium bromide is pumped into the generator chamber. Although the atmospheric chamber is divided into two sections, vapor is still able to travel from one side of the chamber to the other. On one side of the chamber, the saturated lithium bromide solution is dripped over a heat exchanger heated by solar hot water. Through this process, the water is vaporized and thereby removed from the solution. The water vapor flows to the condenser side of the chamber to heat exchanger coils of cool water

that comes from a cooling tower. When the water vapor hits the cool water pipe, it condenses into liquid and drops to the bottom of the tank. Now, the tank has the lithium bromide on one side and the water in the other. The lithium bromide is pumped back to the bottom of the vacuum chamber and the water is sent to be dripped over the chilled water pipe in the vacuum chamber. This cycle will continue as long as the hot water is above 70 °C, and is depicted in the figure below.
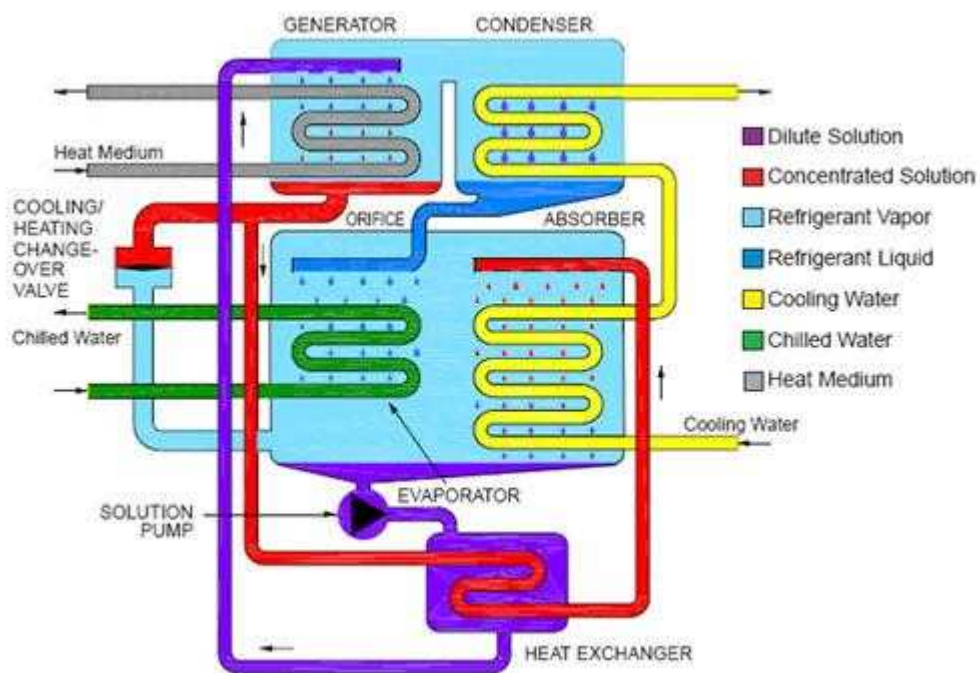
Figure 1.3: Absorption Chiller [1]

To keep the hot water supplied to the absorption chiller above the 70 °C without intermission during the day, 3,000 gallons of water must be cycled from the HWT through the solar heat exchanger and back to the HWT before starting the chiller. This will prevent the absorption chiller from shutting down when there is an obstruction between the collectors and the sun, such as a large cloud or a bird.

1.5   Solar Energy

Solar energy, as applied to buildings is energy that is collected from the sun that is either converted into heat or electricity. Solar radiation, or short-wave radiation, is radiation originating from the sun in the wavelength range of 0.3 to 3 μm [8]. Another term typically used to describe solar radiation is electromagnetic radiation. The wavelengths of 0.3 to 3 μm consist of a part of the Ultraviolet spectrum and part of the infrared range [39].

The amount of solar energy available on Earth is not fully known, therefore scientists came up with a constant called the Solar Constant. The Solar Constant is the energy from the sun, per unit time, received on a unit area of surface perpendicular to the direction of propagation of the radiation, at mean earth-sun distance, outside of the atmosphere [8]. The World Radiation Center uses a Solar Constant value of 1367 W/m^2 [8]. After the solar flux has gone through the atmosphere, the energy received on the ground can be as high 1000 W/m^2 on a sunny day. The reason for the reduction in solar energy is due to some of the radiation being reflected off the atmosphere and clouds, back into space, or some of the radiation being absorbed and diffracted, leading to a shift in the wavelength and a distinct change in direct and diffuse components of radiation. In general, the more clouds and particles that are in the atmosphere, the lower the amount of solar flux that will hit the surface of the Earth.

1.6   Solar Collectors

There are two dominant methods for the collection of solar energy. One is the use of photovoltaic cells to convert the energy into electricity. The second is through solar thermal collectors, whereby the energy is collected and stored in a thermal mass.

Usually at the scale of a building, the thermal mass utilized is a water tank, but can be anything that has the ability to store energy such as air, a reservoir, molten salt or steam for utility-scale systems.
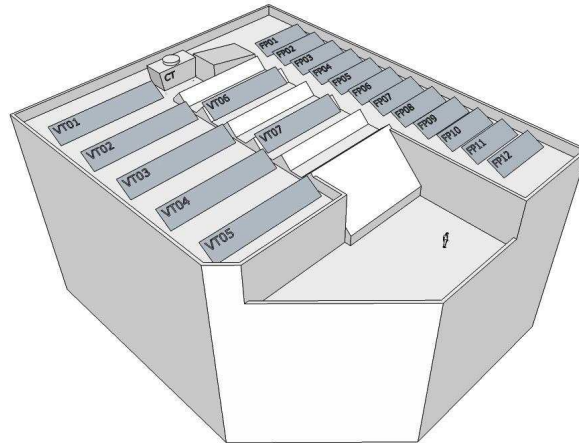
Figure 1.4: Solar collector layout on the roof of the Mechanical Engineering building at UNM. The vacuum tube collector array, labeled VT01-07, consists of five rows of six collectors in series, and two rows of five collectors in series. The flat plate array, labeled FP01-12, consists of 12 rows of seven collectors. The collectors in each row are piped in parallel, arranged in four groups of three collector rows in series. The vacuum tube collectors are Sunda Seido 1-16, the flat plate collectors are Lennox LSC-18 Solarmate.

The solar collection system on the roof of the Mechanical Engineering Building at the University of New Mexico is a solar thermal system. As depicted in Figure 1.2 above, there are two different types of collectors on the roof. The first is an older model, flat-plate collector (Lennox LSC-18) with a net absorber surface area of 1.48 m^2 each. There are 84 of these collectors installed, creating a total surface area of 124 m^2 [2]. The absorber plate consists of a steel plate coated with a black chrome selective surface. Heat is removed by a heat medium (e.g. water/glycol mixture) flowing through 10 copper tubes attached to the plate. The plate is enclosed in a metal case that has a double pane glass lid. The solar radiation passes through the lid and is absorbed by the black metal plate. The enclosure is at atmospheric

pressure and is water tight. As a result, heat is lost through the collector because of convection heat transfer from the plate to the glass cover and between the glass covers, as well as some conduction heat transfer. This was a common type of collector 30 years ago and is still found in use today, although the double layer glass covers are rare. These collectors are positioned at an angle of 25° from horizontal. This is ideal for summer collection given Albuquerque's latitude of 35°.

The newer solar thermal collectors use the same basic principle of collection as the old collectors in that they heat a liquid using a metal plate, but that is where the similarity ends. Vacuum tube collectors (Sunda Seido 1-16) consist of a long metal plate that only contains one enclosed tube which is partly filled with water under a slight a vacuum. The entire plate is enclosed within a vacuum glass tube. Convection heat transfer cannot take place with the absorption plate being surrounded by vacuum, thus keeping the heat loss to a minimum. The fluid within the tube is heated and converted into vapor. The vapor travels up the tube to a metal condenser outside the glass tube that is connected to the inside of the header. The heat from
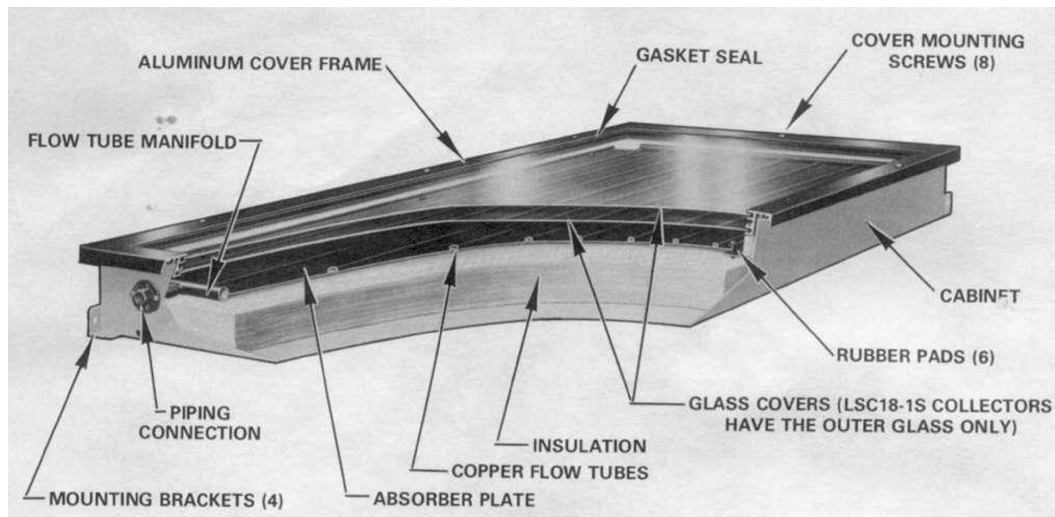
Figure 1.5: Lennox LSC-18 Flat-Plate Collector [2]
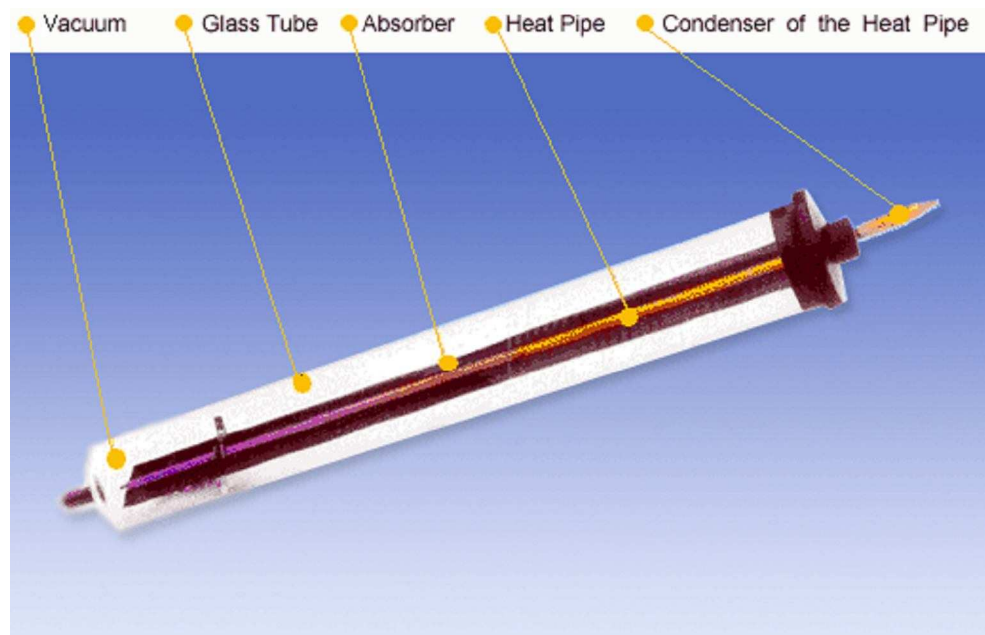
Figure 1.6: Solar vacuum tube collector [3]

the vapor transfers to the water/glycol mixture that is flowing through the header. Once the heat from the steam is transferred, the vapor reverts to a liquid and falls back to the bottom of the tube [4]. This cycle continues as long as solar radiation
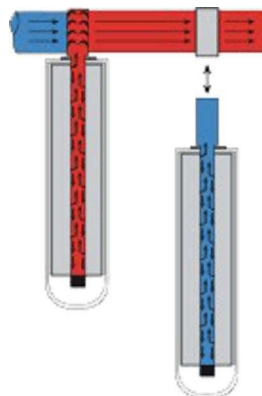
Figure 1.7: Solar vacuum tube collector connecting to a header[4]

maintains a high enough plate temperature. These collectors are positioned at an angle of 35° from horizontal for ideal year round collection. The total absorber surface area of all the vacuum tubes is 108 m^2 [2].

1.7   ReflecTech®

As is evident from the Literature Review, the use of a reflector to redirect solar energy onto collectors is not a new concept. Reflectors of all different shapes and sizes have been used to change the direction or concentration of solar energy to a different location. For this project, the use of rectangular reflectors was selected, because it helps achieve the objective of making the cost as low as possible. Rectangular reflectors make the project an economically viable option for building operators that want to improve their own solar thermal systems. Odd shaped reflectors, or those that have a concave geometry, are more costly.

When the word reflector is used, many people think of a mirror, a piece of glass with a silver application on the back. As discussed in the Literature Review section, many of the researchers used a reflectivity value ranging from 0.8 to 0.88 for simulation modeling and experiments. Although use of a glass mirror may be a good option for reflecting the solar radiation, it has drawbacks. The first is that glass is very fragile and may not hold up over time to the common elements of high winds and hail. The second is that it is very heavy to handle and must be installed in a heavy-duty frame to hold the extra weight of the mirror.

In selecting a reflector appropriate for this project, other reflective materials were considered, such as silver paint and aluminum. As discussed in the Literature Review section, these too have some problems. The first is that both of these materials have a lower reflectivity than a glass mirror, approximately 0.7 and the level of reflectivity drops dramatically for both materials over time. One of the goals of this project

is to install these reflectors only once, without many adjustments or changes after installation. If the reflectors need to be replaced after several years, then the cost of the project will be increased substantially.

Figure 1.8: ReflecTech® Installed in the Field [5]

For this project, the use of a new material called ReflecTech® was selected. ReflecTech® was first created in the late 1990s and later patented in 2006. ReflecTech® Mirror Film is constructed of multiple layers of polymer films with a layer of pure silver to provide high spectral (mirror-like) reflectance while protecting against UV radiation and moisture. It has a pressure sensitive adhesive for application to smooth surfaces. A peel off release liner covers the adhesive until application and a peel off mask protects the mirror surface during processing, handling, transportation, and installation [6].

ReflecTech® was designed to provide a highly reflective surface that would effectively weather the outdoor elements. In 2009, a conference paper [7] was presented on the current tests and the results that were achieved with respect to the material's durability when exposed to the elements. Some of the tests accomplished
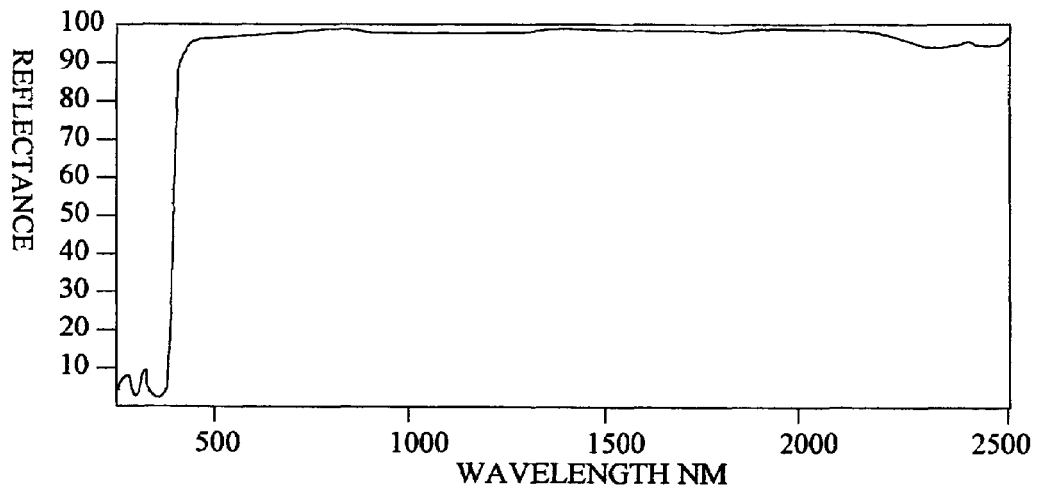
Figure 1.9: Spectral Hemispherical Reflectance of RelfecTech® from Patent [6]

included putting ReflecTech® under ultraviolet light during accelerated testing and under normal outdoor testing, a water immersion test, a high wind test, and a high temperature and high relative humidity test. When the tests were all completed, the material showed very little change in its reflectivity. During a 6 year outdoor
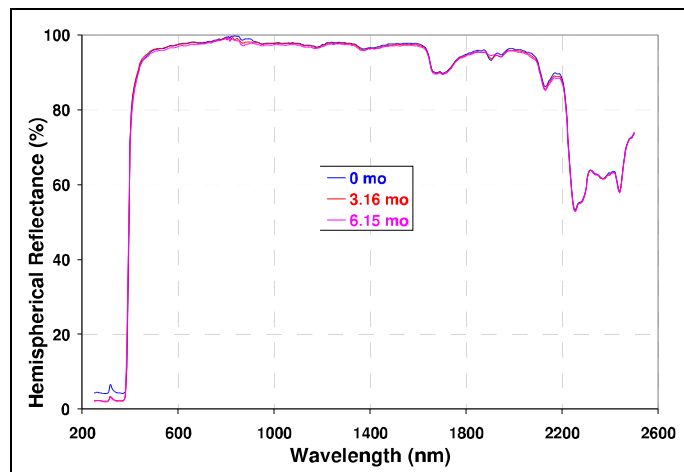
Figure 1.10: Performance of ReflecTech® after an Accelerated Weather Test (6.15 months ≈ 1.5 years) [7]

test in California, the material's hemispherical reflectance across the solar spectrum dropped by less than 1%.

ReflecTech® Mirror Film recently surpassed the 20 year mark demonstrating durability against ultraviolet (UV) radiation using the Ultra-Accelerated Weathering Station (UAWS) at the National Renewable Energy Laboratory (NREL). UAWS is the most accelerated method to determine the long-term durability of a material to outdoor exposure. Natural sunlight is concentrated 50X while sample exposure temperatures are maintained at 30C and 60C to accelerate degradation mechanisms. After receiving the equivalent cumulative UV dose of over 20 years outdoor exposure, no degradation and no loss in reflectance were measured in three replicate samples.

ReflecTech® has many advantages in addition to its weatherability and ease of installation. The solar-weighted hemispherical reflectance of the material is 94% and the specular reflectance is 94% at 660 nm and 25-mrad. This reflectivity is greater than the 80% to 88% levels of reflective materials characterized in previous studies. The material is also cost effective. The cost of the material plus the aluminum backing is less than \$30/m², which is much cheaper when compared to a glass mirror that could cost \$43-64/m² [7]. Therefore, because of its predictability, safety, durability, and performance ReflecTech® was selected for this project.

Chapter 2

Location, Orientation and Assembly of Reflectors

2.1 Selection of Collector Boost Period

The direction of a project can take many different paths given the decisions made along the way. For this thesis, the issue that is being addressed is how to increase solar thermal energy collection during the summer months while minimizing the changes to the system. To meet these goals, and as stated in the introduction, the increased solar flux cannot be much greater than the maximum design load of the solar thermal system already in place. This is an important distinction that sets this project apart from previous studies accomplished on this topic. As presented in the Literature Review section, the goal in the previous studies has been to increase the peak performance of solar collectors. Increasing the peak creates a higher level of solar flux collected during the 2 to 3 hour period around solar noon and requires the redesign of the solar thermal collection system for a higher maximum load. Implementation of such a change could be very costly.

27

Chapter 2. Location, Orientation and Assembly of Reflectors

The only way to increase the solar energy collected while not increasing the maximum design load at any given time, is to have the solar power plateau at the current system's maximum design load. This would increase the total area under the solar power curve mentioned in Chapter 1. In order to create this effect, the reflectors must be oriented to only provide enhancement during the morning and afternoon, but not at solar noon.

There could be two sets of reflectors on top of the Mechanical Engineering Building, one set to increase the collection in the morning and another set to increase collection in the afternoon. Considerations were made to account for the weather in the Albuquerque area before setting up the two sets of reflectors. During the late summer months of July, August, and September a weather pattern develops when warm moisture from the Gulf of Mexico comes into the area which allows thunderstorms to form over the mountains and provide rain for the region. This weather pattern is known as the monsoon season. A typical day during the monsoon season will have clear skies in the morning with some clouds building over the surrounding mountains by midday. These clouds typically develop into thunderstorms by the afternoon or evening.

To determine the effects this weather pattern could have on the design of the mirror booster system, solar flux data were collected from August 3 through August 11 and August 14 through September 16, in 10 minute intervals (see Figure 2.1). The data were then combined to create the graph below, depicting a 24 hour period. In the graph, it can be seen that a relatively solid curve can be defined between the 6th and 14th hour (MDT) of the day, but after 14th hour the curve is not as strong and shows a more spread out collection of data points. This suggests that over the course of a month and a half, the solar flux collected in the morning was more consistent than in the afternoon, which is expected given the monsoon weather pattern previously described. Because of the higher probability of reduced flux due

to clouds in the afternoon, as supported by the data collected, a decision was made to only install the reflectors that would reflect the morning sun's radiation. This would not only provide the best opportunity to increase the collection of solar energy, the cost would be much less than installing two sets of reflectors, thereby supporting the cost effectiveness goal of the project.
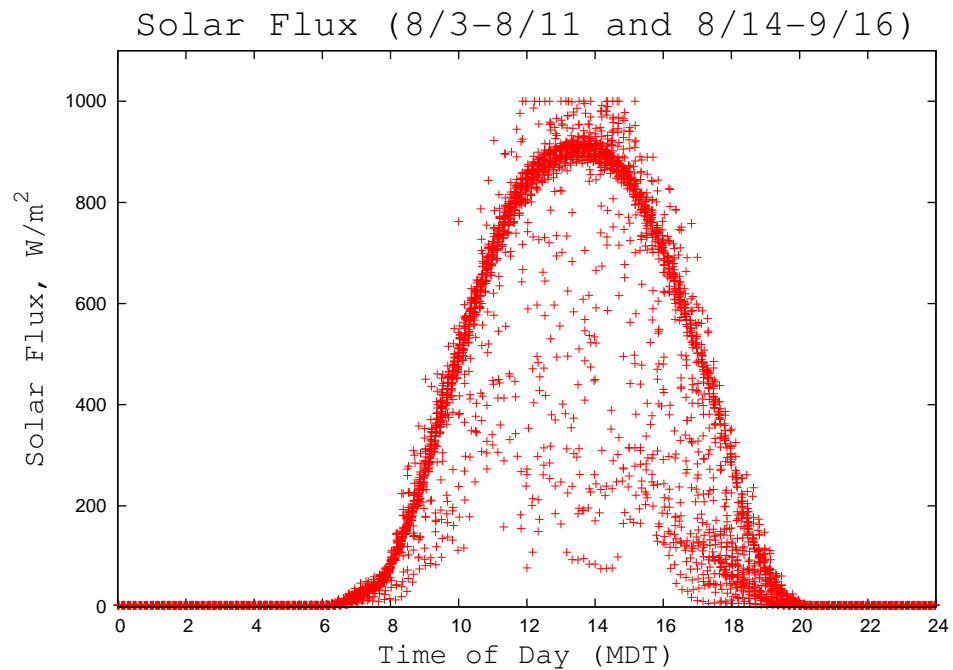
Figure 2.1: Global Solar Flux Data Collected During the Late Summer on a south facing surface at 30° from horizontal

2.2 Scale Model

The first phase of the project involved testing various configurations on a small-scale model. Quantitative evaluation of the configuration's effectiveness was obtained by taking photos of a gray surface that was exposed to direct sunlight and also had reflected sunlight being directed upon it. The use of a gray surface was selected

because its radiation properties are independent of wavelength [8]. The incident energy over the surface was assumed to be uniform, except for the mirror reflection. Given the above, it is possible to take photos of the surface and use image processing software [40] to create a histogram with which to analyze the amount of energy striking it. In order for the data to be comparable between different configurations, the camera settings were identical for each photo taken. This gray surface was placed on a model of a row of vacuum tube collectors at an angle of 35° and was built using a ratio of 12:1.
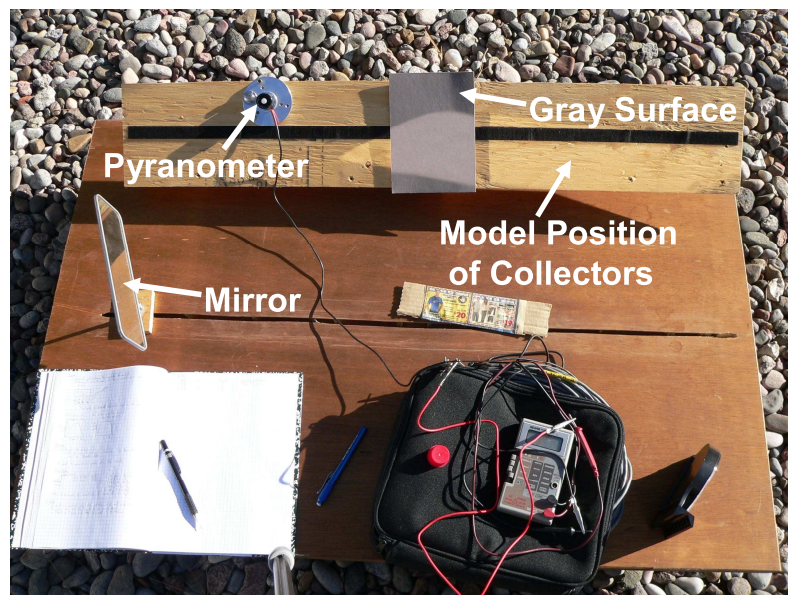
Figure 2.2: Photo of scale model showing the mirror reflecting the sun onto the gray surface while the pyranometer reads the solar flux at an angle of 35°

Histograms were generated (see Figure 2.3) to study the two levels of energy hitting the gray surface resulting from direct solar flux, and from combined direct and reflected. The gray scale has a range of 0 to 255. The higher the gray scale number, the higher the amount of energy on the surface. The peak on the left represents the energy from direct sunlight and the peak on the right is a combination of direct sunlight and reflected sunlight from the mirror. The mean gray scale number for

each peak was taken from the histogram to form a ratio. To find the amount of energy striking the gray surface, a Licor LI-200 pyranometer was placed at the same angle to the sun as the gray surface. For example, in Figure 2.3 the mean gray scale numbers for the peaks are 36 and 69 with a pyranometer reading of 472.32 W/m^2. Therefore, flux impinging on the gray number 36 is 472.32 W/m^2 and the energy hitting the gray number 69 is 905.28 W/m^2. This shows an increase in flux of 92%. Even though this is just an example, the percentage increase in energy striking the gray surface can fluctuate dramatically depending on the type, location, position, and uniformity of the mirror surface. Another factor to consider is the time of day and the position of the sun.
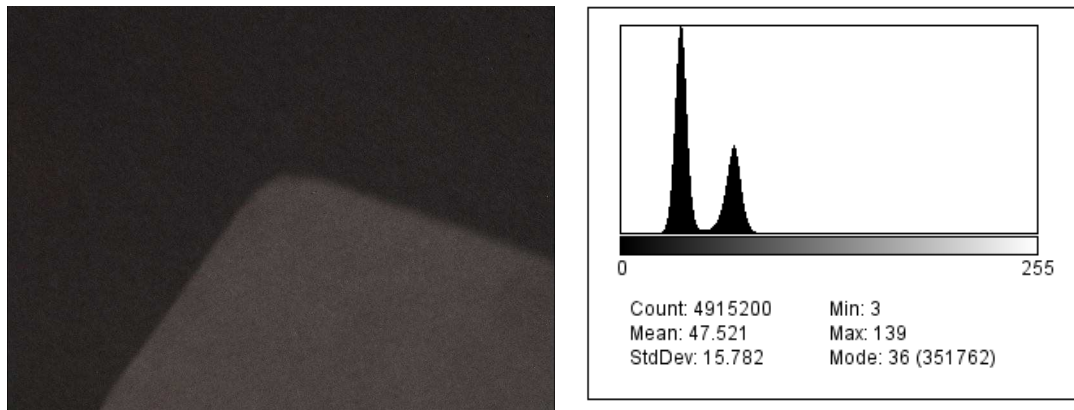
Figure 2.3: Left Image: Photo taken of gray surface, dark gray is receiving direct sunlight and light gray is receiving direct and reflected sunlight. Right Image: Histogram of photo with the peak on the left representing the dark gray surface and the peak on the right representing the light gray surface.

The next step was to find the optimal orientation for the mirrors. There were several considerations, including the number of mirrors, the shading of the mirrors by each other, the location of the mirrors with respect to the solar collectors, and the size of the mirrors. The initial size of the mirrors was to be 1.22m by 1.22m (4 ft by 4 ft) for ease of handling. The best location for the positioning of the mirrors with respect to the collectors was determined to be adjacent to the back of the next row of
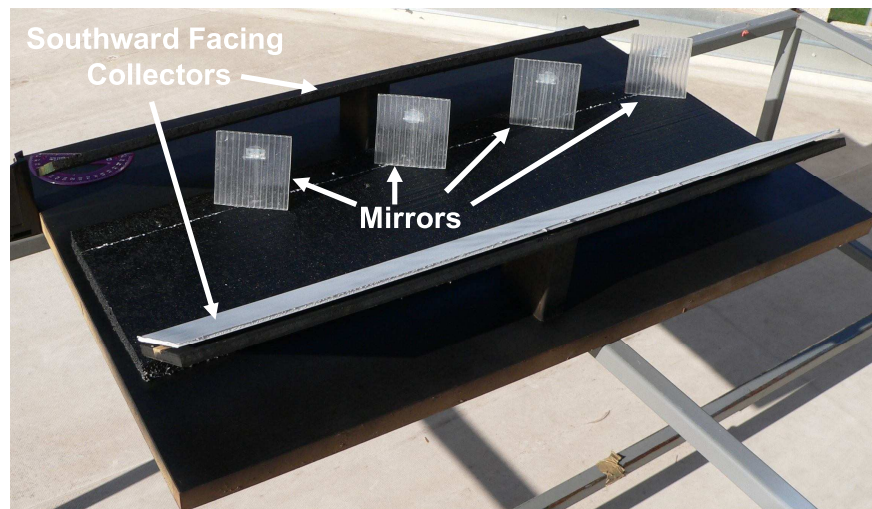
Figure 2.4: Example of Mirror Spacing for Studying Mirror-to-Mirror Shading

collectors to prevent shading during the winter months. This is the reason a second row of collectors was installed on the model, to represent the distance between rows. After observing the model for several days, it was concluded that 6 to 8 mirrors would work best for this solar collection system with the mirrors at an azimuthal orientation of 45 ° with respect to the collectors and a vertical tilt of approximately 15 °.
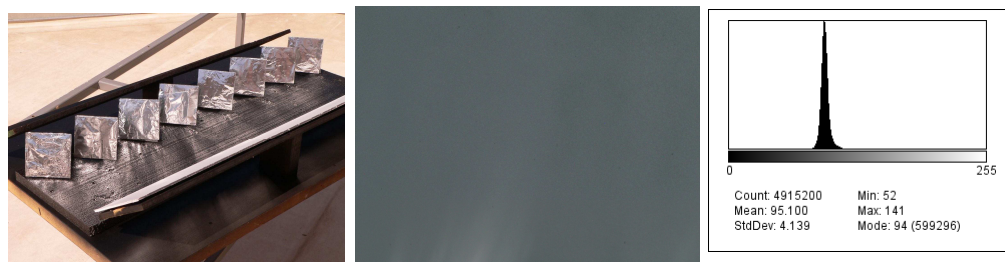
Figure 2.5: Left: 8 aluminum foil mirrors to observe reflections on gray surface. Center: Photo of gray surface with an aluminum mirror reflection taken at 8:30 MDT. Notice very little change in the surface shading. Right: Histogram of photo with no double peak, showing very little aluminum mirror reflection on the gray surface left of the peak.

ReflecTech® was not available at the time of this simulation, therefore aluminum foil was used as a temporary substitute. Observations were made of the aluminum foil with different tilt angles ranging from $10°$ to $20°$ and it was noted that the $20°$ appeared to be the best angle. The limited reflectivity of the foil mirrors did not compare favorably to the glass mirror used to generate previous histograms (see Figure 2.5).

Once the samples of ReflecTech® were installed on the model, there was a clear difference between the ReflecTech® and aluminum foil, as would be expected. Another observation was the amount of reflection that was hitting the base of the model or the roof of the building and not the collectors. The scale model allowed the rough determination of the size, number and position of the mirrors, but it became clear that experiments alone were not sufficient. To realize the full potential of the design, a full scale simulation was needed.
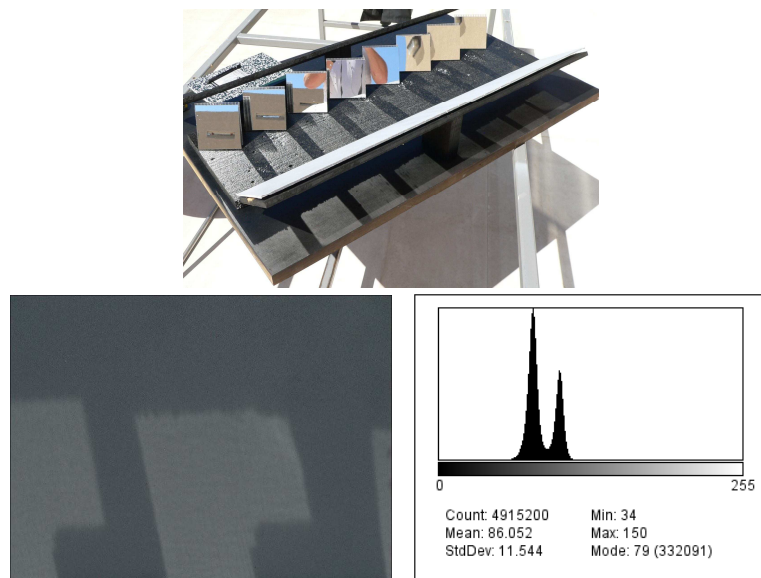
Figure 2.6: Reflection using ReflecTech® at 8:15 MDT

2.3 FORTRAN Simulation

It proved difficult to set up the experiment to account for a specific set of conditions, since the solar path changes every day. With simulation, on the other hand, experiments can be repeated any number of times for any desired conditions. To do this, the program must be written to find the solar radiant power absorbed by the collectors from the sun and the reflection from the mirrors during any given time and day of the year. In order to do this, the code was written to perform the following tasks:
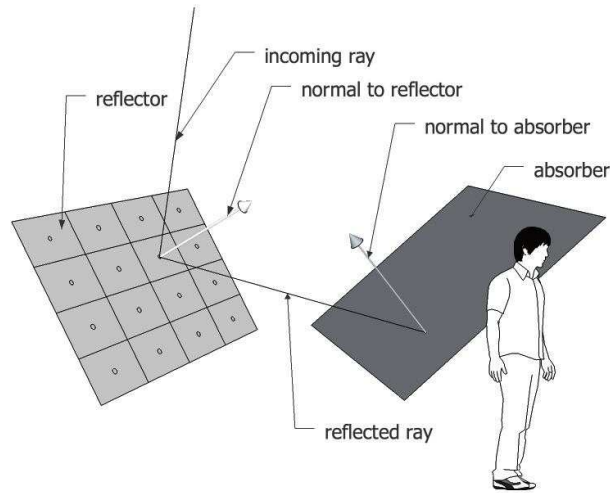
Figure 2.7: Schematic of solar rays striking the collector and the reflector to the collector

1. The surface of the reflector was subdivided into a large number of equally sized rectangles and area A_r. The radiant power P_i impinging on the area element is given by:

$$P_i = A_r G_i \mathbf{d}_i \cdot \mathbf{n}_r, \tag{2.1}$$

where G_i is the incident flux, $\mathbf{d}_i$ is the unit direction of the incoming radiation, and $\mathbf{n}_r$ is the unit normal to the reflector surface. The equations used to locate

the position of the sun at any given time were provided by Duffie and Beckman [8].

2. The ray impinging on the center of each rectangle is reflected using vector geometry. The reflected power P_r is:

$$P_r = \rho P_i, \tag{2.2}$$

where ρ is the reflectance of the mirror surface.

3. The point of intersection of the reflected ray with the plane of the collector surface is calculated.

4. If the point of intersection is within the dimensions of the collector, then it is assumed that the power delivered to the collector is:

$$P_a = \text{IAM}P_r, \tag{2.3}$$

where IAM is the incidence angle modifier, which can be calculated using the components of the reflected ray in the longitudinal and transverse collector directions.

By adding the individual contributions of each area subdivision, the total contribution of the reflectors to the power absorbed by the collector is obtained. The code also calculates the shading from reflector to reflector and reflector to collector. This is important information to finding the size and location of the mirrors and the effect of shading from the reflectors to the collectors during the winter months.

The code is able to calculate the energy collected by the system with or without the mirrors for any desired period of time. Thus, provided that an optimization function exists (e.g. total energy over a specified period) it is possible to optimize design parameter such as position, orientation, number of collectors, etc.

2.4 Prototypes

When designing the framing and mounting system for the mirrors the three major considerations were cost, weatherability, and size of the mirror. The weather in Albuquerque can cover a wide range of temperatures (from below $-20\,°C$ to over $40\,°C$) and wind speeds (over 112km/hr) with precipitation of 240 mm per year, with high winds come dust and dust storms. The size of the mirrors was eventually modified from 1.22m by 1.22m (4 ft by 4 ft) to 1.52m by 1.22m (5 ft by 4 ft) because the ReflecTech® material is manufactured in rolls with a width of 1.52m. The new size would provide enough spacing to eliminate mirror-to-mirror shading when the azimuthal position of the sun, aligned with the normal to the mirror face on June 21, during which the sun reaches its northern most position. This was discovered by using the simulation program.

With these considerations, three prototypes were constructed. The first was based on an extruded aluminum T-section frame assembled using pop rivets and a polycarbonate sheet which was attached to the frame using an outdoor silicon caulking. The second was a pressure treated wood frame assembled using screws and brackets. The polycarbonate surface was attached to the frame using the same outdoor silicon caulking. Polycarbonate is a lightweight, rigid, easy to handle product that provides an ideal surface upon which to apply the ReflecTech®. It can withstand long term exposure to ultra violate light which made it an attractive material to incorporate into the design.

As the first two prototypes were installed and observed for weathering issues during the spring time, which is normally the windiest time of the year in Albuquerque, the silicon caulking was not holding up to the weather exposure, causing the polycarbonate to separate from the framing. It was clear that some changes were needed, possibly including a new design for the frame. The silicon caulking from the

aluminum frame was removed and replaced with a more expensive outdoor adhesive. A third prototype was also created at this point, using 1.9 cm by 3.8 cm (0.75 inch by 1.5 inch) pine lumber. A slot was cut into the length of the lumber to fit the polycarbonate and the ends were cut with 45° chamfers. The frame was assembled using wood glue, staples and 2.5 cm by 7.6 cm strips of sheet aluminum. The lumber was painted to protect it from weathering. After observing the three prototypes for several months, it was clear that the third prototype was going to be the best option. Not only was it the most cost effective to build, it was able to withstand the weather elements during the testing period without observable damage.

Figure 2.8: From right to left: 1st prototype (Aluminum Frame), 2nd prototype (Pressure Treated Lumber Frame), 3rd prototype (Regular lumber made into a slotted frame)

2.5   Assembly

The original plan was to install the reflectors to the back side of the next row of collectors, as seen in Figure 2.10. This changed when the results from the simulation

program indicated that moving the mirrors to a position directly in front of the solar collectors would increase the energy collected from approximately 4% to 14%. This drove a big change to the design of the frame, requiring it to more fully support the now freestanding mirrors, and raised concerns on the shading that might be cast on the collectors during the winter. Despite these obstacles, the decision was made to change the location of the mirrors.
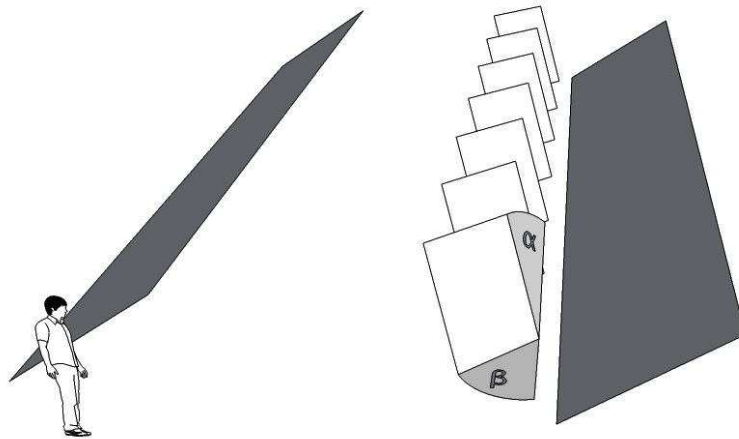
Figure 2.9: Schematic of the mirrors with the vacuum tube collectors, α and β are the orientation angles to the mirrors

Figure 2.10: Photos of mirrors set at $\alpha = 20°$ and $\beta = 42°$ in front of the solar vacuum tube collectors

The base frame was designed using metal framing (Unistrut or similar), metal brackets, nuts, bolts, washers and utilizing mounting pillars already existing on the rooftop. The initial results from the simulation program showed that an orientation defined by $\alpha = 20°$ and $\beta = 42°$ (refer to Figure 2.9) would be the best position for the experiment. Therefore, the first row of mirrors was set up as seen in Figure 2.10. To connect the mirror to the base frame, the use of conduit (metal tubing), L shaped brackets, nuts, bolts and washers were needed. Although polycarbonate was an ideal mounting surface for the ReflecTech®, this design aspect also changed, as the manufacturer would only sell ReflecTech® preinstalled on aluminum sheets for reasons of quality assurance. In the end, this aided in cutting the time required for the assembly of the mirrors as the lamination process that would have been required to mount the ReflecTech® onto the sheet of polycarbonate was eliminated.

A second row of mirrors was installed, with α was changed from 20° to 30° for comparison testing (see Figure 2.11).
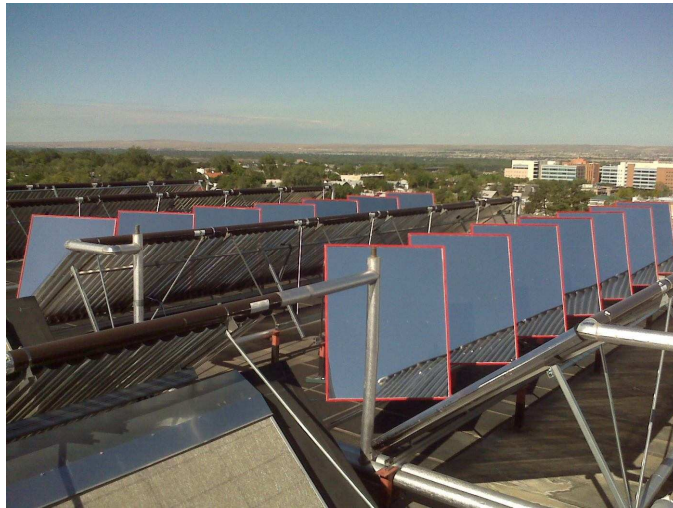
Figure 2.11: Mirrors in the background are set at $\alpha = 30°$ and $\beta = 42°$ and mirrors in the foreground are set to $\alpha = 20°$ and $\beta = 42°$

In designing reflectors for the flat-plate collectors, the location and size were

limited by the minimal space available (see Figure 2.13). As a result, the size of these mirrors is 1.52 m by 0.91 m (5 ft by 3 ft). The angles of the mirrors are $\alpha = 45°$ and $\beta = 6°$. This setup provides higher performance during the late morning, rather than mid-morning as in the case of the vacuum tube collectors, meaning that the constraints on the optimization of the reflectors were the main design driver.
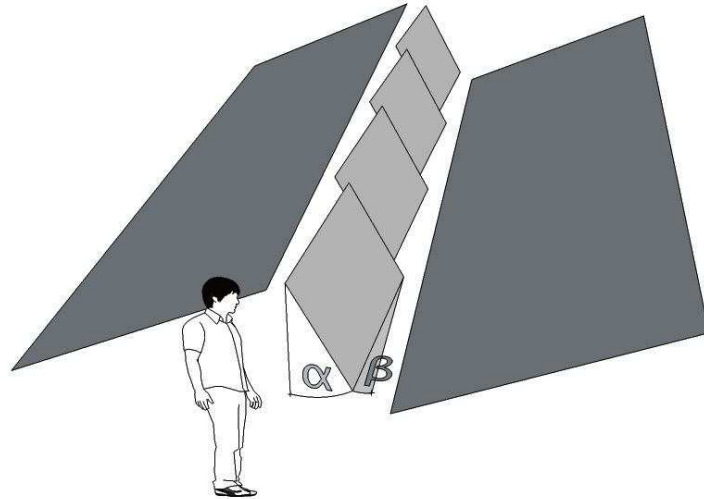
Figure 2.12: Schematic of the mirrors with the flat collectors, α and β are the orientation angles vertical and azimuthal respectively.
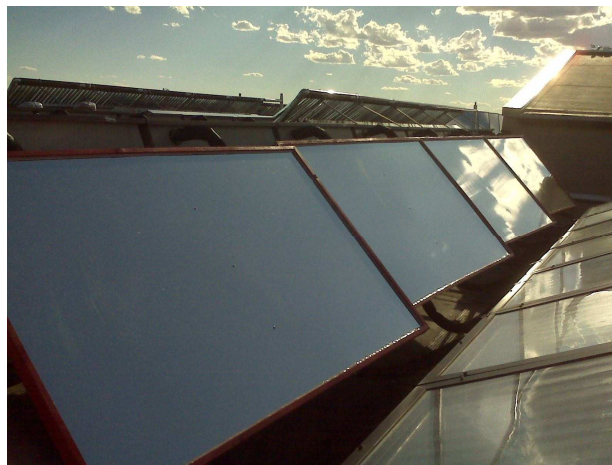
Figure 2.13: Mirrors installed in front of the flat-plate solar collectors

Chapter 3

Experimental Setup and Results

3.1   Test Fixture and Setup

To measure the effectiveness of the mirror/collector system, the flow rate along with the inlet and outlet temperatures of the water/glycol mixture were measured and logged. Also, solar flux data were collected using a Licor LI-200 pyranometer to measure the solar flux at any given time.

To find the temperature of the water/glycol mixture for the inlet and outlet of a given row of collectors, Type T thermocouples were inserted into pressure-temperature test plugs that were already installed in the piping of the solar collection system. A pressure/temperature test plug is a device which allows the insertion of a probe inside a tube while the system is pressurized. The thermocouples were installed at the inlet and outlet points for the rows of vacuum tube collectors with mirrors set at $\alpha = 20°$ and $\alpha = 30°$. An additional thermocouple was installed to collect the outlet temperature for a row of vacuum tubes unaided by mirrors. The flow rate for all three rows of collectors was equalized by using circuit setters. The flow rate was measured by using the system flow meter, an Onicon F-1110

41

turbine device. The voltage output from the Type T thermocouples was collected using an acquisition/switch unit, Agilent 34970A, and converted into °C. The Licor LI-200, placed at the same 35° angle as the vacuum tube collectors, produced a current output that was converted into a voltage by inserting a resistor between the terminals. The voltage was amplified by a factor of 1000 and recorded using the Agilent 34970A. The following equation was used to convert the amplified voltage reading into solar flux:

$$F_s = \frac{V_a \lambda}{\Omega \epsilon}, \tag{3.1}$$

where F_s is the solar flux (W/m^2), V_a is the amplified voltage (Volts) reading from the Agilent 34970A, λ is the conversion of 11,520,000 W/m^2 per Amp, Ω is the resistance (ohms) used which equals 47 ohms, and ϵ is the amplification factor equal to 1000.

The temperature and voltage data were collected on a laptop at ten second intervals. The average data collection time would start at approximately 8:00 am (MDT) and finish around 2:00 pm (MDT).

The testing for the flat-plate collectors was simplified because only one set of mirrors was installed with an orientation of $\alpha = 45°$ and $\beta = 6°$. Type T thermocouples were installed at both the inlet and outlet points for the rows with and without mirrors. The Licor LI-200 was positioned at a 25° angle to match the flat-plate collectors. The flow rates for the flat-plate collectors were also equalized by adjusting the circuit setters.

3.2 Numerical Results

The significance of using a simulation program is that it allows a designer to find the ideal position of the mirrors while minimizing the amount of time needed to set up and make adjustments. In the case of solar energy, simulation is even more essential since a set of desired test conditions may only exist for a few days per year. The program could also be used for other projects with similar design and orientation issues. This simulation was used to optimize the orientation of the mirrors from late spring to mid-summer to early fall, but could be used for any stretch of time. If, instead, the mirrors were to be installed only once with no adjustments to be made, then the mirrors must be set up for optimal performance during June 21 (see Figure 4.1). The results presented in Figure 4.1 were obtained from a simulation in which the size of the mirrors was 1.52m by 1.22m and 7 mirrors in one row. A row of mirrors is located in front of the vacuum tube collectors, as seen in the Figure 2.9.

The graph in Figure 3.1 illustrates the predicted performance of the mirror-collector system as a function of mirror orientation for June 21. The orientation of the mirrors are shown by the angles of α and β. The performance gain, E/E_0, is the ratio of total solar energy collected with the mirrors, E, and the total solar energy collected without the mirrors, E_0. The legend on the right is the ratio of the peak rate of energy collected with the mirrors to the peak energy collected without the mirrors. To avoid severely overloading the glycol circulation system, the ratio of peak power must stay below 1.05, indicated in the graph by dark shading. The optimal configuration is located at the boundary of the dark region of the figure, where the surface reaches the highest elevation. By inspection, this corresponds to α = 20° and β = 42°. The orientation α = 30° and β = 42°, results in a slightly higher peak ratio, but also a higher E/E_0. Both orientations were experimentally tested.

An additional validation of the simulation predictions involved observation of the
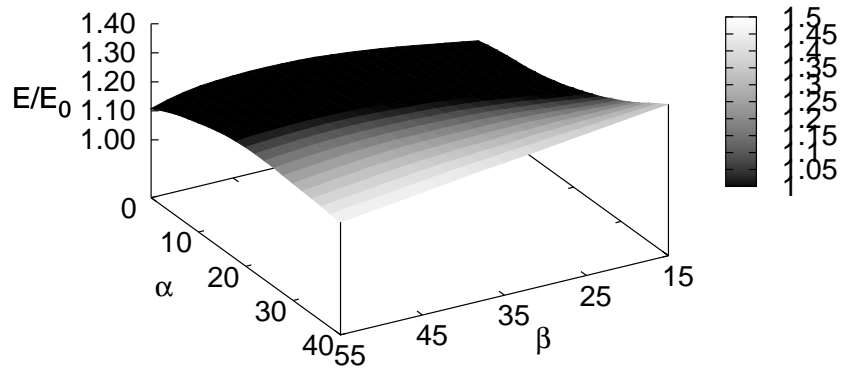
Figure 3.1: Mirror orientation (α & β) with respect to the vacuum tube array, correlated with the ratio of energy collected (E/E_0) and shading of the ratio of peak energy collected on June 21

reflection of the mirrors onto the vacuum tube collectors, accounting for the effect of mirror shading, was evaluated in the simulation program (see Figure 3.2). The graph shows a large area covered by the mirror's reflection at 8:00 solar time, but square notches in the bottom right corner of each reflection illustrate the effect of mirror to mirror shading. At 9:00 solar time, the surface area covered by the mirrors is reduced, but the effect of mirror to mirror shading has been eliminated. The last graph shows even less mirror reflection on the collectors at 10:00 solar time. The results were those desired as the effect of early morning mirror enhancement was indeed being provided to the collectors.

Figure 3.3 shows the collector heat capture rate with no mirrors, mirrors at α = 20°, α = 30° and the corresponding ratio of performance. The graph describing the unaided collectors is similar to the solar flux of a sunny day. This curvature was expected and serves to validate the simulation program. The shape of the graph for the mirrors oriented at $\alpha = 20°$ matches the goal of the project in figure 1.1 with heat capture rate increasing early in the morning and creating a plateau until solar noon. This provides the highest performance gain until 10:15 (MDT), when the

June 8, 8:00 solar time

June 8, 9:00 solar time

June 8, 10:00 solar time
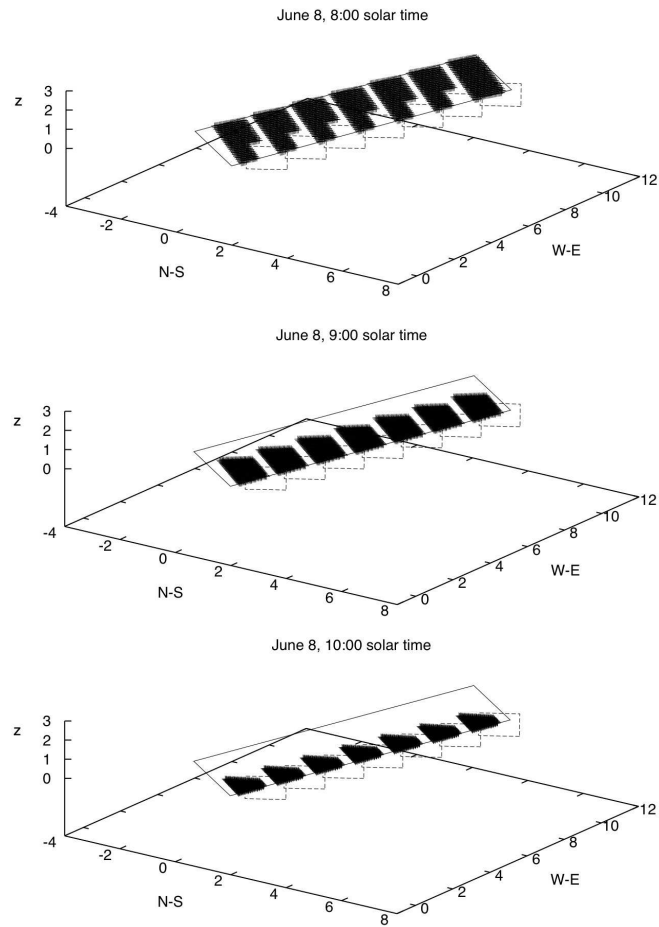
Figure 3.2: Predictions of mirror reflection onto collector surface for mirror orientation $\alpha = 20°$, $\beta = 42°$.

mirrors positioned at $\alpha = 30°$ surpasses at a ratio of 1.9. This means the collectors are gathering 90% more power with the aid of reflectors at 10:15 when $\alpha = 30°$. The mirrors placed at $\alpha = 30°$ provide the largest amount of heat capture rate at 24,000 W from 11:00 to 12:00 (MDT) and the highest overall power when comparing the areas under the curve for no mirrors and mirrors positioned at $\alpha = 20°$.

If the mirrors were installed at $\alpha = 30°$ and $\beta = 42°$, the model predicts a heat capture rate increase of 14% on June 21 and would go over the design load
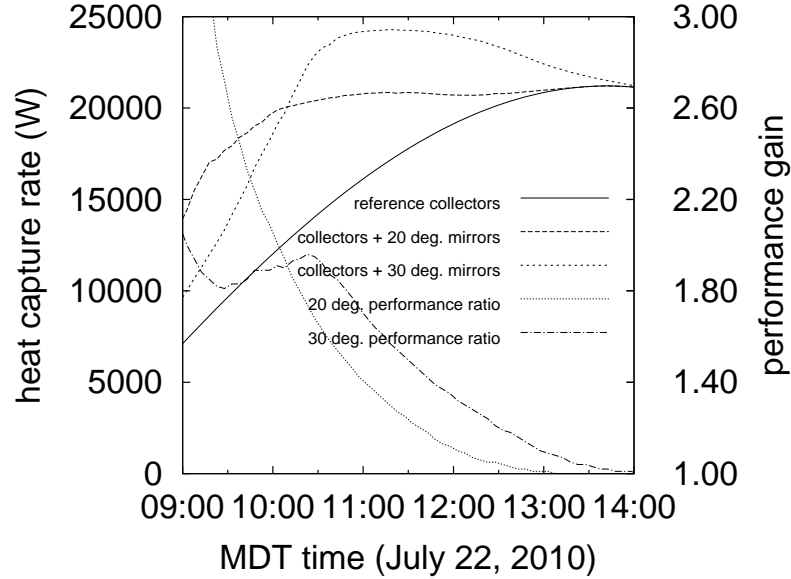
Figure 3.3: Energy capture rate for vacuum tube mirror-enhanced rows and reference row, and in-plane solar flux.

by 8% (noting that the maximum load for 35° collectors occurs in late March and mid September)for approximately 1.5 hours a day. The solar collection system can handle the additional energy by increasing the pump speed for short periods of time. In addition, only 5 of the 7 rows of vacuum tube collectors will be enhanced by mirrors. The following equation was used to find the percentage difference in the design peak load compared to any day of the year:

$$\frac{\Delta P}{P} = 1 - cos(|\Theta - \Phi|), \tag{3.2}$$

where ΔP is the difference of power at solar noon on March 21 and June 21, P is the peak power on March 21, Θ is the zenith angle of the sun on March 21 at solar noon, and Φ is the zenith angle of the sun on a given day at solar noon.

The performance gains generated by the mirrors are very similar in shape after 10:30 (MDT), but are offset by 45 minutes with $\alpha = 30°$ providing a 0.25 higher

performance gain than $\alpha = 20°$ during any given time between 10:30 to 12:30 (MDT). Part of the validation for the simulation is provided when the performance gain drops to 1 at 13:00 (MDT) for $\alpha = 20°$ and at 14:00 (MDT) for $\alpha = 30°$, when the heat capture rate of each oriented mirror is equal to the unaided collectors, since the reflection has shifted away from the collectors.
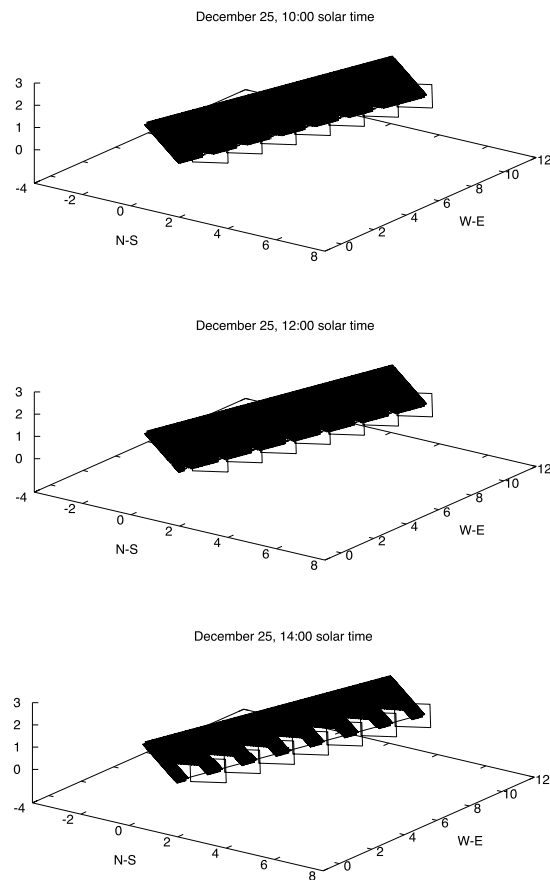
Figure 3.4: Shadows on Christmas day where $\alpha = 30°$, $\beta = 42°$.

Since the reflectors are mounted next to the vacuum tube collectors, an analysis was accomplished to determine the extent of the shading caused by the mirrors during the peak winter season (see Figure 3.4). During the late morning solar hour of 10:00 and the mid day solar hour of 12:00, there is very little shading on the collectors

because the thickness of the mirror frame is the only part facing the sun. At 14:00 solar time, the shadowing increased to cover one-third of the collector's surface area. If the position of the mirrors were $\alpha = 20°$ and $\beta = 42°$, the shadowing would be greater due to the higher position of the collectors. Although experimental data for this scenario have not been generated, the results are logical given the low position of the sun during the winter months.

Figure 3.5 quantify the effect of shading on the collectors and the amount of heat capture rate during the day of December 25. The influence of reflector shading is first noticed at 7:30 solar time when compared to no mirrors. The shading is eliminated for a very brief period at 10:30 solar time and a substantial reduction in energy collected is observed until sunset. A positive result was noticed when the mirrors not only provided reflection, but boosted the energy being collected between 8:15 and 11:00, when compared to unaided collectors. Enhancement resulting from reflection ends at 11:00 solar time. Once again, these results have not been tested experimentally, but provide supportive data for biannual adjustments of the reflectors.
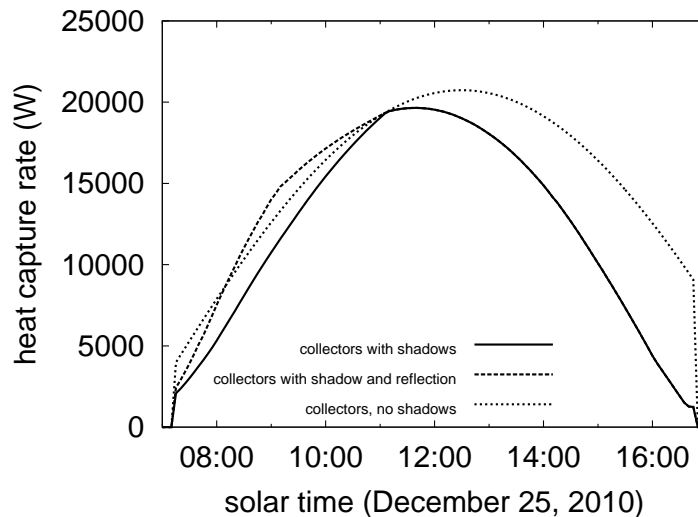
Figure 3.5: Heat capture rate on December 25 where $\alpha = 30°$, $\beta = 42°$.

Using the same procedure as in Figure 3.1, Figure 3.6 was generated for the flat-plate collectors to find the ratio of daily energy captured and the peak rate ratio at different α and β orientations. The best position for the reflectors is at $\alpha = 30°$ and $\beta = 25°$, but as stated earlier, the β angle is limited to an angle less then 7° because of geometric constraints. Therefore, the position of $\alpha = 45°$ and $\beta = 6°$ was selected, giving a E/E$_0$ value of 1.3 and the peak ratio of 1.25. Less than half of the energy collected by the total solar collection system is from the flat-plate collectors and the peak ratio for the vacuum tube array happens around 10:00 solar time. Because the peaks for the vacuum tube and the flat plate arrays are non-coincident, the total system peak ratio would be approximately 1.12 and would not provide an excessive strain to the total system.
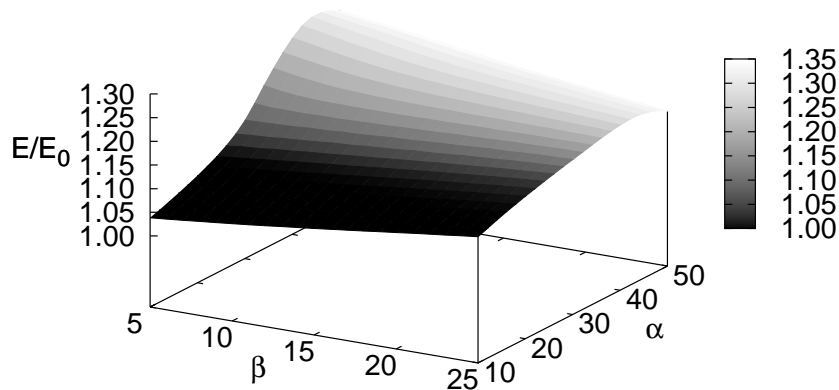
Figure 3.6: Mirror orientation (α & β) to the flat-plate array, correlated with the ratio of energy collected (E/E$_0$) and shading of the ratio of peak energy collected on June 21

A shadowing graph was not generated for the flat-plate collectors because the selected orientation ($\alpha = 45°$ & $\beta = 6°$ and size (1.52m by 0.91m) of the mirrors would not create shading during the winter months. The heat capture rate and performance gains of the mirrors on the flat-plate collectors are shown in Figure 3.7. The peak heat capture rate of the unaided and aided collectors happens at

13:30 and 13:00 (MDT), respectively, and the performance gains are much lower for the flat-plate collectors when matched with the vacuum tube collectors. There are two reasons for the large difference in performance gains realized by each of the collectors. First, the flat-plate array simulation was conducted during the late summer as opposed to mid summer for the vacuum tube array. Secondly, the peak effect of the mirrors occurs in the late morning for the flat-plate collectors, when the unaided collectors are near peak performance. The vacuum tube collectors get mid morning enhancement when the unaided collectors are at 50% of peak performance.
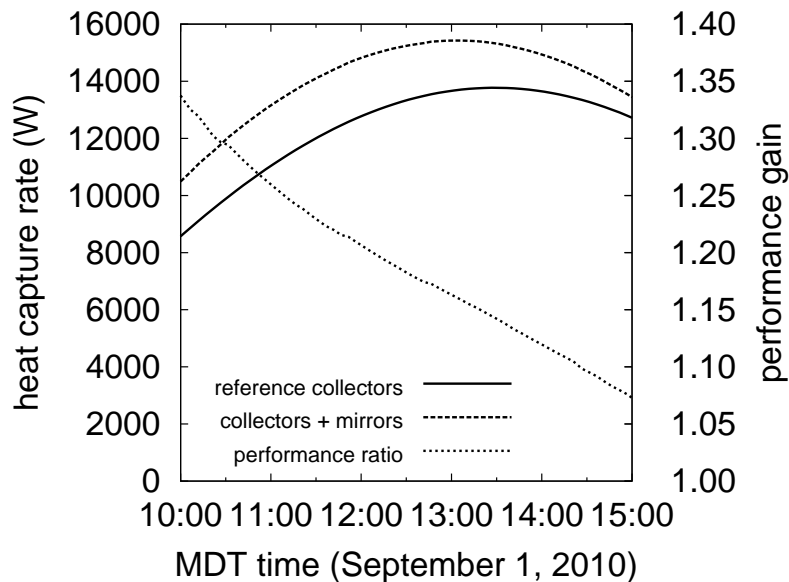
Figure 3.7: Energy capture rate for flat-plate mirror-enhanced rows and reference row, and in-plane solar flux.

In the next section, experimental results are presented. Model predictions will be validated using these results.

3.3   Experimental Results

To validate the accuracy of the simulation model, tests were conducted on days modeled in the previous section. Inspection of the experimental data plotted in Figure 3.8 reveals clear weather conditions, except for a period of partly cloudy skies between 10:00 and 10:30 (MDT). From 11:45 to noon, there is an apparent large spike in the heat capture rate. This is not caused by clouds, as indicated by the constant solar flux during this period, but took place because of the activation of the absorption chiller. The system reached steady state again shortly after 12:00. It is important to note that the heat capture rate for $\alpha = 20°$ reaches its peak at approximately 11:00 and remains constant, except for when the absorption chiller turns on, until it converges with the heat capture rate of the unaided array of collectors.

The reflectors positioned to $\alpha = 30°$ produce an increase in heat capture rate as high as 13% as compared to the reference array between the hours of 11:00 to 13:00 and begin to converge with the unaided and the $\alpha = 20°$ collectors. The simulation model shows a heat capture rate increase of 14% which supports the accuracy of the program. As mentioned earlier, this output is acceptable because of the short period of 7% higher designed maximum energy collected with only 5 of the 7 rows of collectors receiving solar enhancement.

The overall heat captured increased as compared to the unaided vacuum tube collectors by 9% for $\alpha = 20°$ and 12% for $\alpha = 30°$. These values were calculated by integrating the heat capture rate over the entire day. It is interesting to note that the shape of the graph is very similar to the simulated model, but the absolute values for the heat capture rate are off by a factor of 1.5 to 2. This is because the model treats the surface of the vacuum tube collectors as one solid area, when in reality, there are thin strips of spacing between the vacuum tubes that do not have a collecting surface.
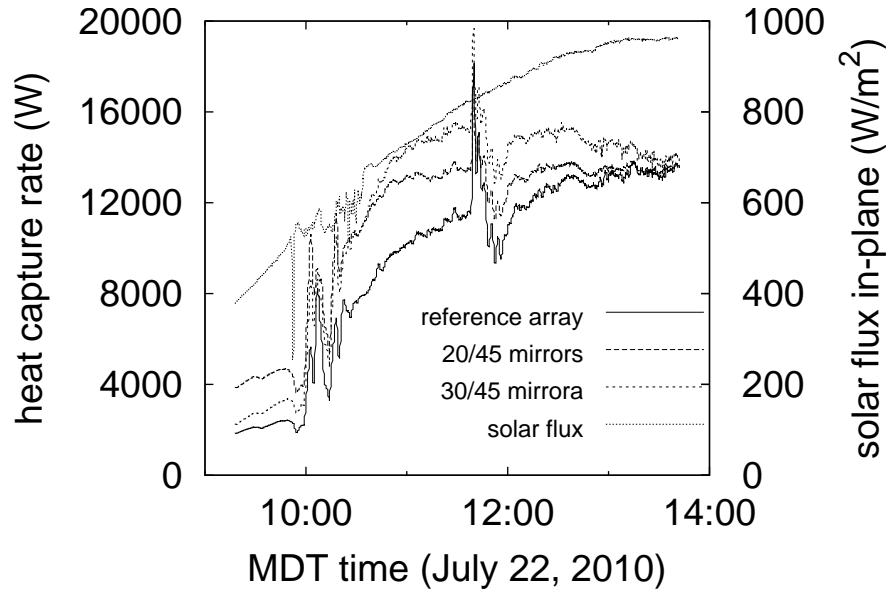
Figure 3.8: Energy capture rate for vacuum tube mirror-enhanced rows and reference row, and in-plane solar flux.

To conduct the same test for the flat-plate collectors, the flow rate of the water/glycol mixture needed to be adjusted for the mirror enhanced collectors to be equal to an unaided row of collectors. By covering the mirrors all day, calibration was conducted to produce identical flow rates. As seen in Figure 3.9, the flow rate was not adjusted until 11:45, when morning clouds cleared. The flow rates for both sets of collectors remained constant until after 14:00 when clouds came over the collectors. Note also that there was no spike in heat capture rate around 11:45 like that seen in the vacuum tube test. This was because the absorption chiller was down for maintenance upgrades.

Once the flow rate calibration was complete, the mirrors were uncovered and the test was conducted again the next day (see Figure 3.10). During the period from 10:00 to 15:00, the total energy captured was computed by integrating the thermal energy capture rate with respect to time. The total energy gained for the unaided
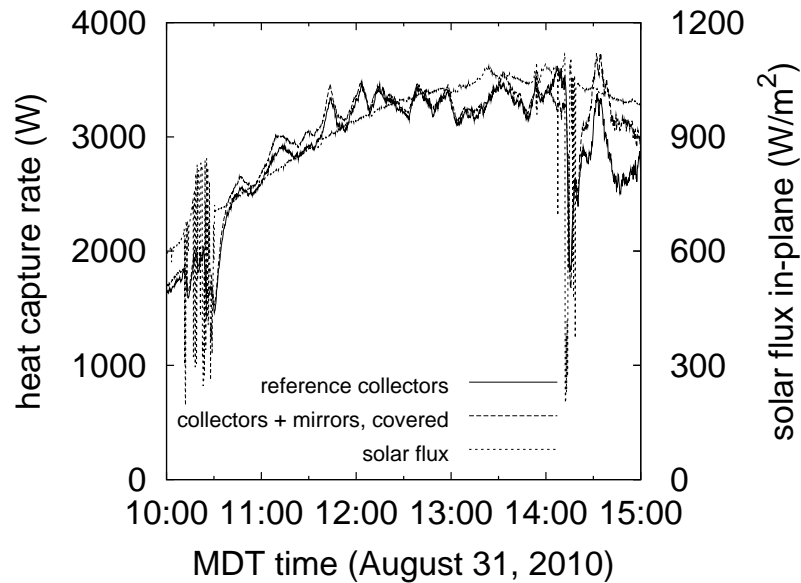
Figure 3.9: Energy capture rate for the test and reference collector rows, with covered mirrors, for flow balancing, and in-plane solar flux.

collectors and the mirror-enhanced collectors was 52.37MJ and 58.66MJ, respectively. This corresponds to an increase of 12% with a peak performance at 12:00, which is an hour before solar noon. During the course of the entire day, the energy captured with the aid of the mirrors increased by 14%.

The peak heat capture rate for both mirror-boosted row and unaided row of collectors occurred at around 12:00 (MDT), while the solar peak in the plane of the collectors occurred at 13:30. This could be explained by the solar collection system being partly shut down for maintenance upgrades, with all of the collectors in the system covered except for those being tested. Collector efficiency gradually decreased with increasing fluid temperature, causing an early peak in heat capture rate. As a consequence, the system temperature never reached the set point, and the flow rate was constant, at the minimum set value.

Another observation is the level of heat capture rate was much lower in reality
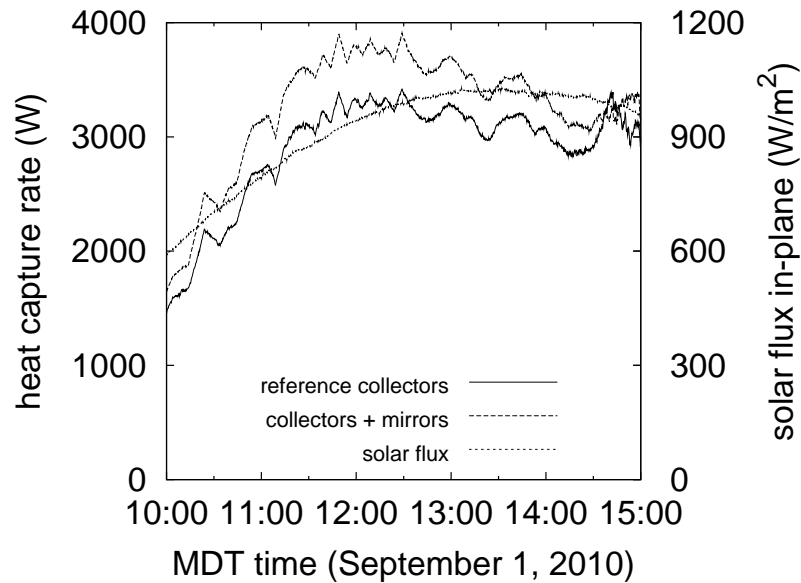
Figure 3.10: Energy capture rate for mirror-enhanced row and reference row, and in-plane solar flux.

than in the simulation by more than a factor of 3. This could be caused by the sunlight being reflected onto the collectors and bouncing off the glass cover, and therefore not being absorbed. For the flat-plate collectors, IAM was unknown and could not be applied to the simulation model. Other factors could be that the testing was conducted on one out of the three rows per set, but the covered collectors still lose heat and reduce efficiency and the effective collector area is much smaller than the area in the model. Even with these discrepancies, the depiction of the model and experimental graphs are very similar. With modifications to the model and when all the collectors are uncovered, the results should be very close for future experiments.

Chapter 4

Cost Analysis and Economics

When developing a new energy efficiency product, there are many factors to consider from a company perspective, such as the cost to build and install, cost to build after being streamlined into production, payback for the customer and efficiency improvements for the customer.

When designing the mirrors used in the present work, a lot of background work was necessary before building the prototypes so that the final cost could remain within budget, especially given the unexpected increase in the cost of the mirror panels. The time spent to build a scale model of mirrors and observe the reflections at different times during the morning and the time to write the code for the simulation program can to be considered as an investment into the new product. The time spent during the conceptual development was not recorded. However, the time needed to assemble and install the mirrors and the prices of all the materials are known. Considering only the cost of materials and the time needed to assemble/install a mirror, the total for one mirror and base frame was $294.83. The cost to build and install an entire row of 7 reflectors was $2,063.78.

As stated earlier, three prototypes were built and weather tested for several
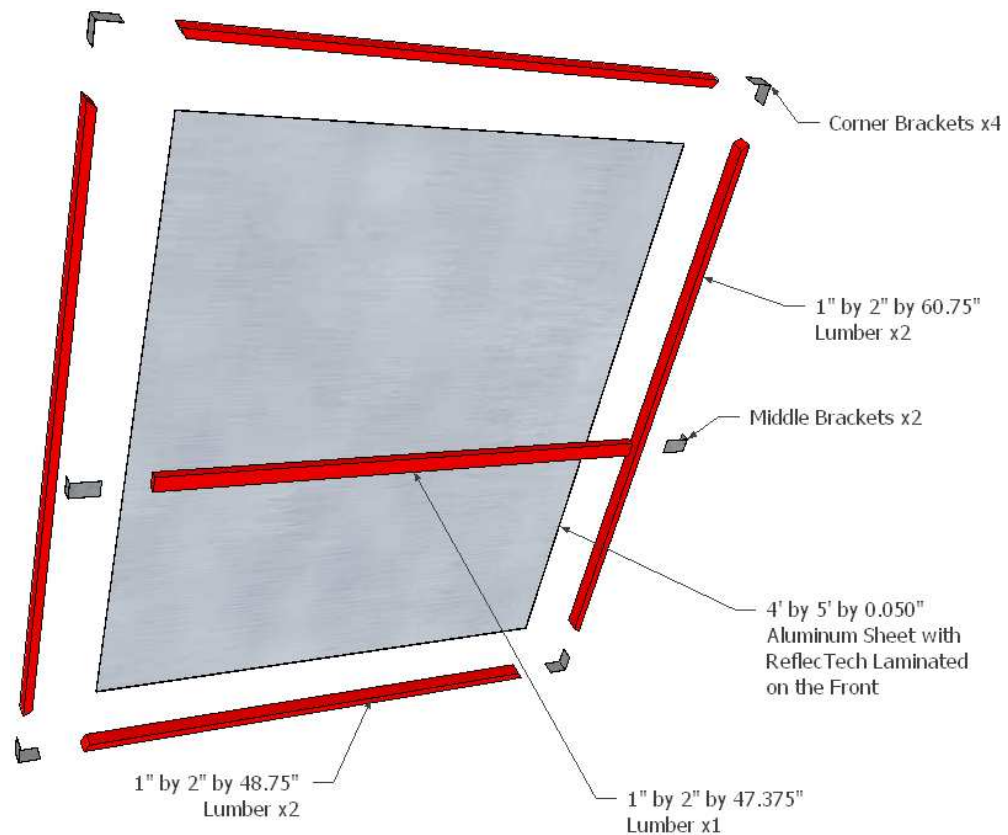
Figure 4.1: Explode View of the Mirror Assembly

months. The third prototype was selected for the reflector assembly, because of its design and low cost in materials. The framing was made from a cheaper 1 inch by 2 inch by 8 feet nominal cut pine, compared to pressure treated wood and extruded aluminum T-section stock from the other prototypes. The lumber was cut into lengths of $60\frac{3}{4}$ inches and $48\frac{3}{4}$ inches with a $45°$ chamfer on each end (see Figure 4.1). A $\frac{3}{8}$ inch deep grove was cut on the long axis of the wood to allow 0.050 inch thick sheet of aluminum with laminated ReflecTech$^®$ to be secured in the framing assembly. The other prototypes have the polycarbonate surface adhered to the frame which caused failures during weather testing. A $47\frac{3}{8}$ inch board was cut and installed to the middle of the frame for structural integrity. The lumber was spray painted

for weather protection and assembled around the sheet of aluminum with wood glue and thin strips of 2.5 cm by 7.6 cm sheet metal formed into brackets and installed with staples (see right side of Figure 4.2). In addition to the brackets, the middle board was secured to the aluminum sheet by 5 screws (see Figure 4.3). The lining of the frame was sealed with silicone caulking and let dry for 12 hours to prevent water damage.
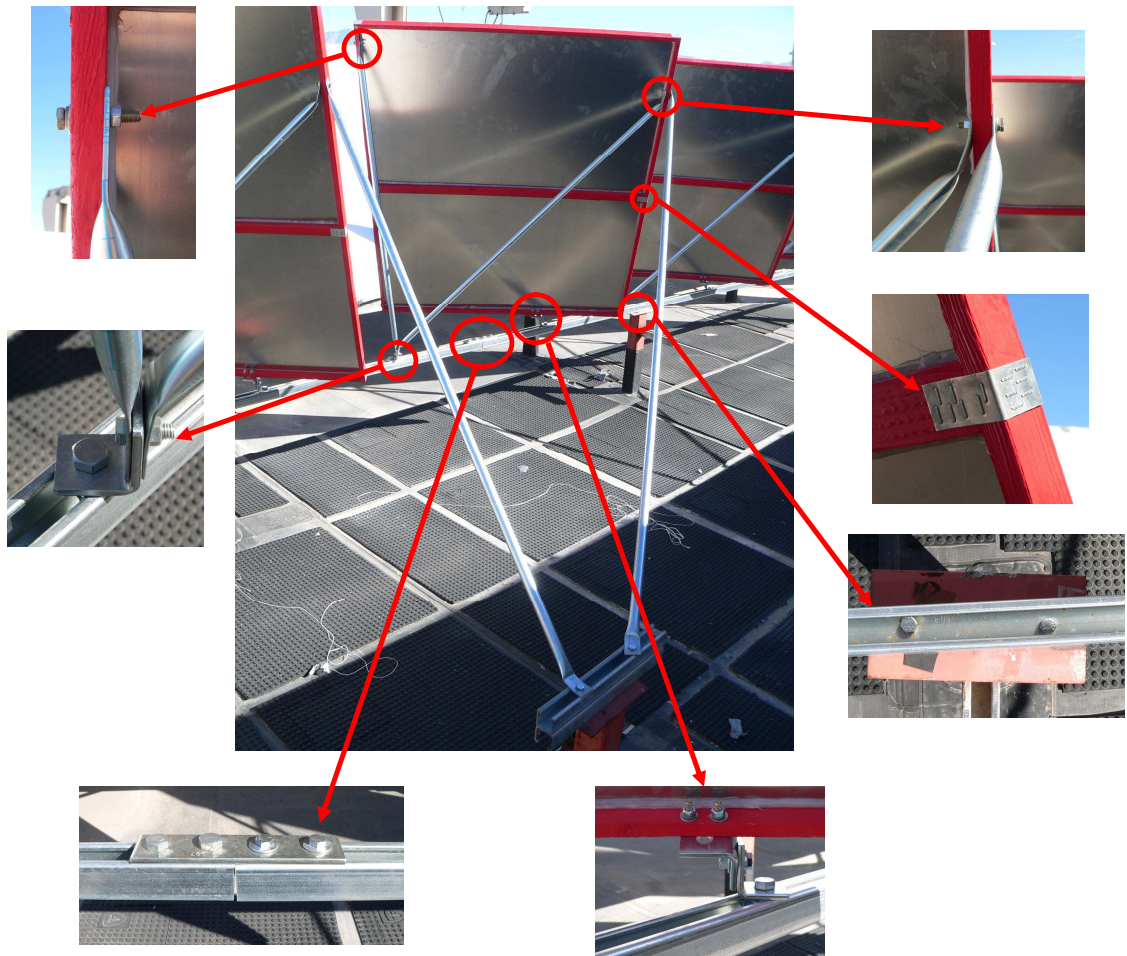
Figure 4.2: Installation of Mirror to Base Frame and Base Frame Assembly

As seen in Figure 4.2, the base frame used eight existing 0.75 m long pillars for each row of reflectors. A continuous length of $1\frac{5}{8}$ Unistrut framing was bolted to
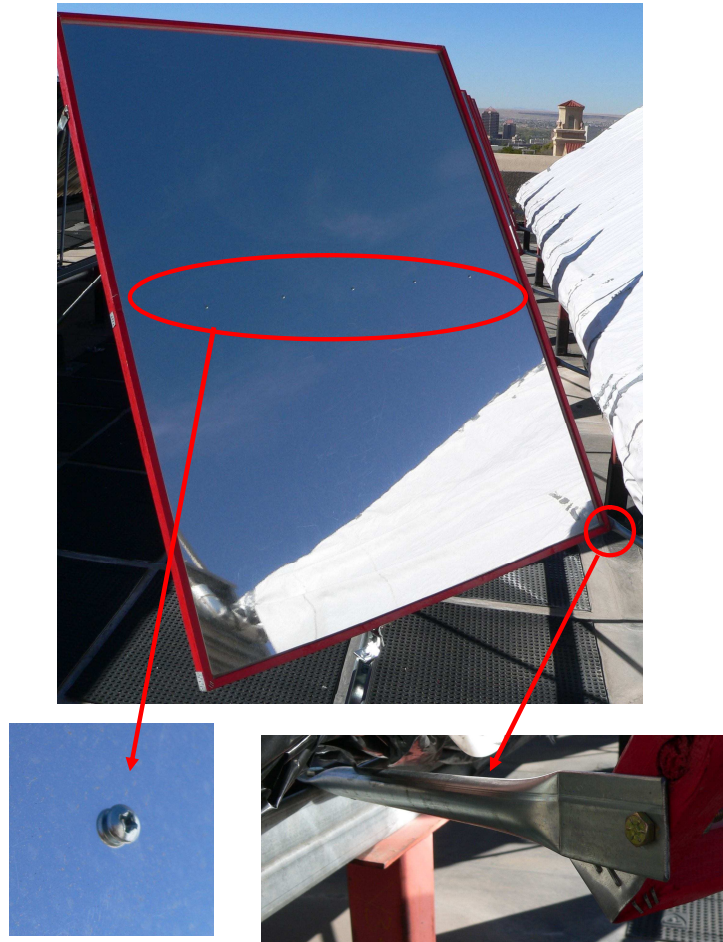
Figure 4.3: Front of mirror showing location of 5 screws to secure reflector to back cross board and forth support bar

existing supports. The framing was connected together with 4-hole brackets. $1\frac{5}{8}$ inch channel back-to-back Unistrut framing was installed on top of the back four pillars. Five $\frac{1}{4}$ inch holes were drilled into the reflector frame as connection points to the base frame. The reflector was attached to the base frame with L-shape brackets and machined $\frac{3}{4}$ inch conduit. The conduit was cut into standard lengths of 16 (see Figure 4.3), 52 and 63 inches with the ends flattened and drilled with $\frac{3}{8}$ or $\frac{1}{4}$ inch holes to connect the reflector to the base frame with hardware. The fourth piece of conduit was cut to a custom length depending on the location of the reflector with

Chapter 4. Cost Analysis and Economics

respect to the back row of pillars.

The breakdown of costs to build the reflectors and the base frame can be seen in tables 4.1 and 4.2. Two challenges arose, finding the lowest prices and finding materials and components manufactured in the United States of America (USA). The funding for this project came from a United States Department of Energy ARRA (American Recovery & Reinvestment Act) program, requiring that all materials and components must be made in the USA. Common materials such as hardware and lumber were purchased at higher prices and longer lead times because of the requirements. A large portion of the budget was consumed when making the purchase from ReflecTech® because of the unforeseen lamination requirement onto sheets of aluminum. The price of ReflecTech® alone could be reduced from \$22.60/m^2 to \$18.84/m^2 if quantities over 5,574 m^2 are purchased [41]. The labor cost was for a Installation & Maintenance Technician I in the Albuquerque area [42] which includes base salary and benefits.

To build a mirror required first time set ups, such as setting up the circular saw, finding a location to spray paint the lumber, and locating an assembly area. These were steps that were needed, but only for small scale manufacturing. Depending on the level and design of manufacturing, there are several methods to produce the reflector framing. Injection molding could create plastic sections of the frame in 1 to 30 seconds with no additional trimming or deburing. Another process is foam molding were a foaming agent is mixed with a plastic resin to expand from 2 to 50 times its original size. If the design were to bend all four sides of the aluminum sheet to create a frame, then roll bending, cold-roll forming or press brake could be applied. High-pressure flexible-die process or hydroforming could also bend the edges of the aluminum sheet in 1 to 3 minutes. With the reduced tool cost of hydroforming, this process is great for prototype or low volume production (approximately 10,000 identical parts) [43].

Table 4.1: Break Down Cost to Build a $259.43 Mirror

Materials	Cost (USD$) per Item	Quantity	Total Cost (USD$)
Reflectech®	137.49	1	137.49
$\frac{3}{8}$ bolt	0.15	6	0.90
90 deg bracket	1.77	3	5.31
$\frac{3}{8}$ washer	0.07	2	0.14
$\frac{3}{8}$ spring nut	0.80	4	3.20
Red Spray Paint	3.44	0.75 can	2.58
Silicone Caulking	5.97	0.75 tube	4.48
Phillips #6 Screws	0.0397	5	0.20
Staples	0.002376	72	0.17
$\frac{3}{4}$ inch Conduit	0.03127	211 inch	6.60
$\frac{1}{4}$-20 bolt	0.152	5	0.76
$\frac{1}{4}$ flat washer	0.0235	5	0.12
$\frac{1}{4}$ lock washer	0.0329	5	0.16
$\frac{1}{4}$-20 nut	0.0333	5	0.17
1 inch x 2 inch lumber	0.0103125	266.5 inch	2.75
Sheet Metal Brackets	0.05	6	0.30
Labor	31.37	3	94.11

If the process were designed for mass production, the sheet of aluminum could go through a three step system. Step 1 is stamp/punch the installation holes or slots on the sheet. Step 2 is laminating the ReflecTech® onto the aluminum sheet. Step 3 is run the sheet through a press brake die to bend the edges. Assume the variable cost to outsource the three manufacturing steps is $55.00 per reflector. The price of the high volume ReflecTech® and the aluminum sheets with shipping is $80.00 per reflector. The fixed cost for the initial set up of the machines is $300.00.

The following equation can be used to find the cost per reflector as the unit volume increases:

$$u(x) = \frac{a}{x} + b, \tag{4.1}$$

where $u(x)$ is the average unit production cost in USD per unit, a is the fixed cost in USD, b is the variable cost in USD, and x is the unit volume of production [44].

Table 4.2: Break Down Cost to Build a $247.77 Base Frame

Materials	Cost (USD$) per Item	Quantity	Total Cost (USD$)
4 hole bracket	3.20	4	12.80
$\frac{5}{8}$ Ch Unistrut	1.85	37 ft	68.45
$\frac{5}{8}$ Ch BTB Unistrut	4.94	4 ft	19.76
$\frac{3}{8}$ bolt	0.15	32	4.80
$\frac{3}{8}$ washer	0.07	32	2.24
$\frac{3}{8}$ spring nut	0.80	16	12.80
$\frac{3}{8}$ nut	0.09	16	1.44
Labor	31.37	4	125.48

Using equation 4.1, table 4.3 was generated to show as the volume of production increase, the cost per unit decrease at an expediential rate. After building 100 reflectors, the cost per reflector ($138.00) is 53% of the original prototype ($259.43). Reducing the cost of the base frame is more difficult, because each solar collection system is located in a different environment. The design of the base frame would be custom depending on the slope and available mounting points on the roof.

Table 4.3: Volume Production vs Unit Cost

Unit Volume	Cost (USD$) per Unit
1	435.00
10	165.00
100	138.00
1,000	135.30
10,000	135.03

An additional modification to the reflector design is to cut the aluminum in half and installed hinges to fold the mirror during the non-enhancement season. The final manufactured reflector might resemble the image in figure 4.4.

When deciding whether to install or not install the reflectors, a payback period calculation can be generated as seen in Table 5.4. The payback period calculation tells how long an investment requires to break even on its return when dividing the
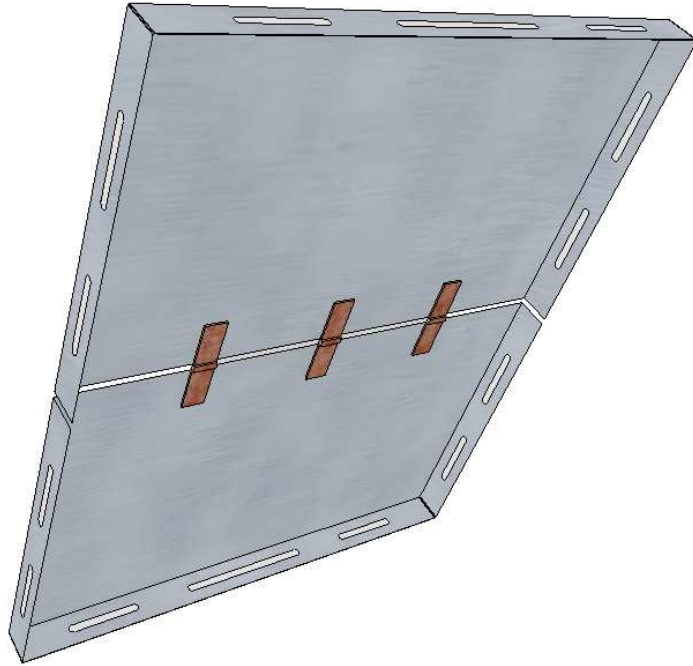
Figure 4.4: Possible mass production reflector with folding option for minimal adjustment time to eliminate winter shading on the collectors.

initial cost by the uniform annual benefit [9]. The initial cost for installing reflectors on the ME Building was $20,000.

The uniform annual benefit UAB can be calculated by the following:

$$UAB = C(P)(T)(D), \tag{4.2}$$

where C is the cost of electricity ($/kWhr), P is the power saved by using the absorption chiller (kWhrs), T is the time the absorption chiller would run extra with the reflectors (hrs), and D is the number of days per year receiving the benefit.

To keep the calculations similar, the Time-Of-Use (TOU) during on-peak hours plan was selected for commercial customers during on-peak hours for several electric companies in the region. On-peak hours were normally 11:00 to 19:00 hours. During

on-peak hours is when the current system's absorption chiller would run an additional 1.5 per day with the aid of the reflectors. The power saved was calculated subtracting the power used at the UNM Physical Plant to run a chiller ($\approx$14kW) from the power used for the absorption chiller ($\approx$4kW), showing a savings of 10kW. The number of days a year the absorption chiller would run was assumed at 245 (March 1 to October 31). As expected, the higher the cost per kWh, the lower the payback period.

Table 4.4: Payback for $20,000 Worth of Mirrors

Southwestern Electrical Companies	On-Peak Cost ($/kWhr)	Payback (Years)
UNM Plant	0.076	71.61
PNM [45]	0.077	70.38
Tucson Electric Power [46]	0.223	24.41
Pacific Gas & Electric (A-1) [47]	0.225	24.23
Pacific Gas & Electric (A-6) [47]	0.453	12.01

Lastly, when comparing the cost to install a row of vacuum tube collectors ($\approx$\$18,000) to a row of 7 reflectors and base frame (\$2,063.79), the reflectors cost 11.4% of the vacuum tube collectors and provide an increase of 12% in energy collected. Testing for the vacuum tube and flat-plate collectors was preformed in late July and late August, respectively. If the testing for both collectors was preformed around June 21, the performance gains could be 1.2 for the vacuum tube collectors and 1.3 for the flat-plate collectors. Also, the tests were done on mostly clear sunny days, not days with cloudy afternoons, so the energy gain throughout the day could go up 5% to 10%. If the mass reproduction cost of the reflectors plus the original cost of the base frame are \$1,192.98 (\$181 per mirror/frame) and compared to the vacuum collectors, the reflectors are 5.9% of the collectors cost with a 20% gain in energy. This would provide a more appealing offer to potential customers.

Chapter 5

Discussion And Conclusions

5.1 Discussion

The components of the HVAC system connected with the solar energy used to heat and cool the building was a 150 kW$_t$ system, costing roughly $400,000. This cost includes the piping, pumps, storage tanks, absorption chiller and the cooling tower, as well as the solar collectors, which themselves account for approximately $150,000. The installation of the mirrors on the roof of the building, for both the flat-plate and vacuum tube collectors, required $20,000 or approximately 5% of the total system cost. As mentioned earlier, the cost of the mirrors can be expected to drop dramatically when manufactured in bulk versus a build for the prototype design. Therefore, we estimate that the total cost of the installation of the mirrors to the system could go from 5% to 2% of the total system. These mirrors simply expand the period of use for the absorption chiller by 1.5 hours per day during the cooling season and require no additional costs for upgrades in the system and only very little to no maintenance. The single drawback is that the reflectors may require additional upkeep with bi-yearly adjustments to prevent shading in the winter months. However,

the cost of this operation could be made minimal by suitable design of the mirrors (e.g. by using a folding geometry).

Both the flat-plate and vacuum tube collectors handled the increase in energy successfully. It was expected that the flat-plate collectors would handle the localization of solar flux striking the surface. The experimental results show that heat pipe designs can handle highly localized "hot spots" resulting from the mirror reflections and transfer the additional heat to the condensers in the header.

The quality and design application of the mirrors can change the output and effectiveness of the total solar collection system. The mirrors that were selected were of a high grade polymer reflective material, with an initial reflectivity of 94%, which was not designed for this type of application, but rather for the more demanding concentrating utility scale systems. The durability and ease of handling of the material also made it an attractive material. If other reflective materials were used, such as polished aluminum or glass mirrors, the long term results of solar performance enhancement to the collectors would diminish.

The location of Albuquerque is considered to be a high altitude desert and requires both heating in the winter and cooling in the summer. The higher quality vacuum tube collectors were installed at the ideal year-round angle of 35°, but the flat-plate collectors were positioned at 25° to provide more energy to cool the building. With the current orientation of the solar collectors, the system provides 90% of the energy for heating and 35% for cooling. This shows a demand for more energy with the aid of reflectors in the cooling season. With the local summer weather pattern of relatively clear skies in the morning and cloudy conditions in the afternoon, the positioning of the mirrors for morning collection enhancement was selected. If the location was instead along the coast where morning fog is common and later burned off to create sunny afternoons during the summer, then an afternoon enhancement would be a better application for the solar collection system.

For an existing or new solar thermal system, the spacing between the rows of panels may be limited and not ideal for additional collectors. The installation of reflectors will utilize all empty spaces to generate an increase in energy. This is a cheaper option compared to changing the layout of the roof and purchasing more collectors. Also, after redesigning the solar collector layout, the mirrors can still be installed in tight locations as was seen for the flat-plate collectors in this project.

The issue of cost for electricity in the region needs to be considered if the designer is looking at a return on investment. The cost of utilities is very low in Albuquerque, but in other areas of the world, the price can increase by a factor of five and create a quicker return. The mirrors could make the difference between the installation or no installation of a new solar thermal system (e.g. the amortization period could be reduced, say, from 30 to 24 years). For an existing solar thermal system, the mirrors could be installed for the entire system, part of it, or not at all, depending on the return rate. At the same time, the architect may not want mirrors installed in locations seen from the ground. If the reflectors are placed in the ideal orientation, the total solar cooling cost could be reduced by approximately 20% which will make the payback much shorter.

5.2   Conclusions

A reflective surface to enhance a solar thermal collector is not a new idea, but many previous studies used mirrors to increase energy collection during the peak time of day. This method is not appealing for an existing solar collection system because the pumps and piping would need to be resized to handle the large increase of solar energy and would diminish a tight budget. Increasing the energy collected during off-peak hours would eliminate additional costs and would extend the collection period of the day when the system is normally underutilized.

The proper orientation of the mirrors was first studied by building a 12:1 scale model of two rows of vacuum tube collectors. The vacuum tube collectors were studied first because their year-round orientation provided the best potential for boosting energy and they had a larger area between rows to work in, compared to the flat-plate collectors. Different quantities, sizes, orientations, and reflective materials were studied using the model. A gray surface, pyranometer and a histogram program were used to test different reflective materials. ReflecTech® was selected as the reflective material to be installed because of its high reflectivity of 94% and durability under the severe weather conditions in Albuquerque.

After studying different configurations using the scale model, a rough design was generated for the number, size, and orientation of the mirrors for a row of vacuum tube collectors. It became clear that a computer simulation model was needed to determine the optimal orientation of the mirrors. Using the simulation model, the ideal mirror orientation was found to be $\alpha = 20°$ and $\beta = 42°$, but the distance from the mirror to the collector needed to be much closer, which boosted the energy collected from 4% to 14% in the simulation model.

With the size of the mirrors determined, three prototypes were assembled and installed on the roof for several weeks during the windy season. After being exposed to the elements, the spray painted lumber frame assembly with metal brackets and staples showed to be the most promising. A small production of 14 mirrors soon began with the wooden framing going around the already laminated reflective material on sheets of aluminum. The first row of mirrors were oriented at $\alpha = 20°$ and $\beta = 42°$ and the second row were at $\alpha = 30°$ and $\beta = 42°$ for comparison testing and to observe if the system could handle an energy boost closer to solar noon.

Testing consisted of 3 rows of vacuum tube collectors, one with no mirrors, one with the mirrors at $\alpha = 20°$ and $\beta = 42°$, and one with the mirrors at $\alpha = 30°$ and $\beta = 42°$. The temperature for the inlet and outlet for each row was recorded in

10 second intervals along with the flow rates and solar flux. The results showed an increase in heat captured of 9% when $\alpha = 20°$ and 12% when $\alpha = 30°$ over the course of the entire day in late July. With this information, 35 mirrors were installed for 5 rows of vacuum tube collectors at $\alpha = 30°$ and $\beta = 42°$ which allowed the absorption chiller to run an additional 1.5 hours per day.

As for the flat-plate collectors, the spacing was very limited for the placement of the mirrors. The simulation model generated an ideal orientation of $\alpha = 30°$ and $\beta = 25°$, but $\alpha = 45°$ and $\beta = 6°$ was the only position possible. Testing was the same as the vacuum tube collectors and the results showed a 14% increase in heat captured over the course of the day on September 1.

The cost to build and install all of the mirrors for the system was 5% of the total solar collection system. In addition to the low cost, the heat captured increased by 12% (vacuum tube collectors) and 14% (flat-plate collectors). This shows that additional energy can be collected for a relatively low price without straining the existing solar collection system.

There are several lessons that can be taken from this project. First, the unfortunate fact of a solar thermal system is that no two systems are alike. The time spent upfront conducting a simulation program is a must when determining the proper position for installing the mirrors. The constraints on the collector's orientation and size, the geographic location, the purpose for the additional energy and the spacing allotted for the mirrors are all critical factors that need to be addressed before proceeding with a project.

The simulation program used generated the location of the reflectors and the possible performance output that was validated at certain times to provide confidence in using the computer model for the rest of the year. But the only way to truly validate the model in the long run is to continue tests and observations throughout

the entire year with the actual system. After studying the results from the simulation model and the actual testing, there are several modifications that could be made to the program that might serve to increase its accuracy, such as:

1. An accurate accounting of the absorber area

2. Accurate collector performance characterization (IAM, etc.)

3. Accurate characterization of the normal and diffuse components of solar radiation

4. Weather statistics

The selection and proper installation of reflectors is an important aspect in the durability and longevity of the enhancement design. The reflectors from ReflecTech® were selected because of their high quality and broad spectrum of outdoor reflective applications. The cost for assembling these reflectors was preformed at a prototype level of production. If these mirrors were assembled at a high volume manufacturing level, the cost of the assembly would go down and the overall quality of the product would increase. Changing the design of the reflectors to have a folding option would eliminate any shading in the winter and could be a minimal part of a biannual maintenance inspection.

The next steps for the ME solar collection system would be to complete the installation of mirrors for the flat-plate collectors, modify the computer simulation program, observe the winter shading effect of the mirrors on the collectors and observe the additional run time of the absorption chiller during the next cooling season.

The use of flat-plate reflectors to enhance a solar thermal collection system is not a new concept, but the idea of increasing the total energy gathered during the entire day without surpassing the design load of an existing system is a different application.

Chapter 5. Discussion And Conclusions

There are many solar thermal collection systems used today, but if the user wants to increase the energy collected and has limited space for the improvement, then the use of reflectors for off-peak enhancement is an attractive solution.

Appendices

Appendix A

Simulation FORTRAN code

```fortran
      module surf_data
!
      integer :: nsurf
      integer :: ncase
      integer :: nx
      integer :: ny
      double precision,dimension(:,:,:,:),allocatable :: xs
      double precision,dimension(:,:),allocatable :: xc
      double precision,dimension(:,:),allocatable :: normal
      double precision,dimension(:,:),allocatable :: horiz
      double precision,dimension(:,:),allocatable :: vert
      double precision,dimension(:),allocatable :: w
      double precision,dimension(:),allocatable :: h
!
      end module surf_data
!
!----------------------------------------------------------------------
!
      program mirrors
!
! calculates additional radiation gain by collectors
! from several reflector surfaces
!
      use surf_data
      implicit none
      integer start,stop,time,interval,cases
      double precision,dimension(3) :: sundir
      double precision,dimension(3) :: reflecdir
      double precision,dimension(3) :: orig
      double precision :: intensity
      double precision :: base_heat_rate
      double precision :: heat_rate
      double precision :: rad1,rad2
      double precision :: x1,x2
      double precision :: eff1,eff2
```

```
        double precision :: area
        double precision :: ratio
        double precision :: baseheat
        double precision :: totalheat
        double precision :: peakheat
        double precision :: peakbase
        double precision :: diffrens
!
! read time file
        open(unit=11,form='formatted',file='time_def.txt')
        read(11,*) start,stop,interval
        close(11)
! process surface information
        call surf_pre_proc
!
! loop through orientation cases
        caseloop: do cases=1,ncase
        call surf_proc
!        write(6,*) 'reflections'
!
! loop through time increments as specified by <interval>
        baseheat=0. ! initialize total heat collection for specified time interval
        totalheat=0.
        peakbase=0.d0
        peakheat=0.d0
        timeloop: do time=start,stop,interval
!          write(6,*) time
! calculate direction of solar radiation
!        time=17366400+43200-0*3600
        call sun_direction(1.d0*time,sundir)
!
! calculate power increase with mirrors
        call reflect(sundir,base_heat_rate,heat_rate)
        eff1=0.d0
        eff2=0.d0
        x1=1.d6
        x2=1.d6
        area=w(1)*h(1)
        rad1=base_heat_rate/area
        rad2=heat_rate/area
        if (rad1 > 0.d0) then
         x1=(90.55-30.0)/rad1
        end if
        if (rad2 > 0.d0) then
         x2=(90.55-30.0)/rad2
        end if
        eff1=0.75-2.04*x1-0.009*x1**2*dabs(rad1)
        if (eff1 < 0.d0) eff1=0.d0
        eff2=0.75-2.04*x2-0.009*x2**2*dabs(rad2)
        if (eff2 < 0.d0) eff2=0.d0
        if ((base_heat_rate*eff1) > 0.d0) then
         ratio=(heat_rate*eff2)/(base_heat_rate*eff1)
        else
         ratio=0.d0
        end if
        diffrens=heat_rate-base_heat_rate
!        write(6,*) time,base_heat_rate,heat_rate,eff1,eff2,ratio,diffrens
        if ((base_heat_rate*eff1) > peakbase) peakbase=base_heat_rate*eff1
```

Appendix A. Simulation FORTRAN code

```
       if ((heat_rate*eff2) > peakheat) peakheat=heat_rate*eff2
       baseheat=baseheat+base_heat_rate*eff1*interval
       totalheat=totalheat+heat_rate*eff2*interval
!
       end do timeloop
       write(6,*) baseheat,totalheat,totalheat/baseheat,
     >            peakbase,peakheat,peakheat/peakbase
!
! deallocate appropriate arrays
!
       deallocate(xs)
!
       end do caseloop
       close(11)
!
!      call sun_direction(1.d0*time,sundir)
!
       end
!
!-------------------------------------------------------------------
!
       subroutine reflect(incoming,base_hr,heat_rate_out)
!
       use surf_data
       implicit none
       integer i,m,n,p
       double precision,dimension(3) :: a
       double precision,dimension(3) :: b
       double precision,dimension(3) :: incoming
       double precision,dimension(3) :: reflecdir
       double precision,dimension(3) :: dist
       double precision,dimension(3) :: origin
       double precision,dimension(3) :: intersect
       double precision :: dot
       double precision :: scale
       double precision :: hcomp
       double precision :: vcomp
       double precision :: base_hr
       double precision :: heat_rate_out
       double precision :: power1
       double precision :: power2
       double precision :: surf_patch
       logical :: shadow
!
! calculate base intercepted power
!      write(6,*) 'reflections'
       a(1)=normal(1,1)
       a(2)=normal(1,2)
       a(3)=normal(1,3)
       b(1)=-incoming(1)
       b(2)=-incoming(2)
       b(3)=-incoming(3)
       dot=a(1)*b(1)+a(2)*b(2)+a(3)*b(3)
       base_hr=1000*w(1)*h(1)*dot  !! assuming dimensions in SI units, in Watts
       if (base_hr < 0.d0) base_hr=0.d0
       heat_rate_out=base_hr
       do i=2,nsurf
       surf_patch=w(i)*h(i)/(nx*ny)
```

74

```
!       write(6,*) 'surf_patch',surf_patch
! assuming flat surface, compute direction of reflected ray
        dot=incoming(1)*normal(i,1)+incoming(2)*normal(i,2)
     >     +incoming(3)*normal(i,3)
!        write(6,*) 'dot=',dot
        power1=-1000.d0*surf_patch*dot
        if (power1 < 0.d0) power1=0.d0
        if (incoming(3) > 0.d0) power1=0.d0
!        write(6,*) 'power',power
        reflecdir(1)=incoming(1)-2*dot*normal(i,1)
        reflecdir(2)=incoming(2)-2*dot*normal(i,2)
        reflecdir(3)=incoming(3)-2*dot*normal(i,3)
        do m=1,nx+1
         do n=1,ny+1
          origin(1:3)=xs(i,m,n,1:3)
          shadow=.false.
! check for interference of incoming ray with surface i+1
        p=i+1
        if (p <= nsurf) then
! calculate distance from source to center of p
        dist(1)=origin(1)-xc(p,1)
        dist(2)=origin(2)-xc(p,2)
        dist(3)=origin(3)-xc(p,3)
        scale=(dist(1)*normal(p,1)+dist(2)*normal(p,2)+
     >          dist(3)*normal(p,3))/
     >         (incoming(1)*normal(p,1)+incoming(2)*normal(p,2)+
     >          incoming(3)*normal(p,3))
         dot=(incoming(1)*normal(p,1)+incoming(2)*normal(p,2)
     >       +incoming(3)*normal(p,3))
!        write(6,*) 'scale=',scale
!        write(6,*) origin
!        write(6,*) origin-incoming
!        write(6,*) origin
!        write(6,*) origin+reflecdir
! point of intersection
        intersect(1)=origin(1)-scale*incoming(1)
        intersect(2)=origin(2)-scale*incoming(2)
        intersect(3)=origin(3)-scale*incoming(3)
!        write(6,*) intersect
! component parallel to horizontal on surface p
        a(1)=intersect(1)-xc(p,1)
        a(2)=intersect(2)-xc(p,2)
        a(3)=intersect(3)-xc(p,3)
        b(1)=horiz(p,1)
        b(2)=horiz(p,2)
        b(3)=horiz(p,3)
        hcomp=dabs(a(1)*b(1)+a(2)*b(2)+a(3)*b(3))
! component parallel to vertical on surface p
        a(1)=intersect(1)-xc(p,1)
        a(2)=intersect(2)-xc(p,2)
        a(3)=intersect(3)-xc(p,3)
        b(1)=vert(p,1)
        b(2)=vert(p,2)
        b(3)=vert(p,3)
        vcomp=dabs(a(1)*b(1)+a(2)*b(2)+a(3)*b(3))
        if ((hcomp <= (w(p)/2.d0)).and.(vcomp <= (h(p)/2.d0))) then
          shadow=.true.
!        write(6,*) 'shadow'
```

```
          else
!          write(6,*) 'no shadow'
          end if
!          stop
! check for interference of reflected ray with surface p+1
          p=i+1
! calculate distance from source to center of p
          dist(1)=origin(1)-xc(p,1)
          dist(2)=origin(2)-xc(p,2)
          dist(3)=origin(3)-xc(p,3)
          scale=-(dist(1)*normal(p,1)+dist(2)*normal(p,2)+
     >          dist(3)*normal(p,3))/
     >          (reflecdir(1)*normal(p,1)+reflecdir(2)*normal(p,2)+
     >          reflecdir(3)*normal(p,3))
          dot=(reflecdir(1)*normal(p,1)+reflecdir(2)*normal(p,2)
     >          +reflecdir(3)*normal(p,3))
!          write(6,*) 'scale=',scale
!          write(6,*) origin
!          write(6,*) origin-incoming
!          write(6,*) origin
!          write(6,*) origin+reflecdir
!          stop
! point of intersection
          intersect(1)=origin(1)+scale*reflecdir(1)
          intersect(2)=origin(2)+scale*reflecdir(2)
          intersect(3)=origin(3)+scale*reflecdir(3)
!          write(6,*) intersect
! component parallel to horizontal on surface p
          a(1)=intersect(1)-xc(p,1)
          a(2)=intersect(2)-xc(p,2)
          a(3)=intersect(3)-xc(p,3)
          b(1)=horiz(p,1)
          b(2)=horiz(p,2)
          b(3)=horiz(p,3)
          hcomp=dabs(a(1)*b(1)+a(2)*b(2)+a(3)*b(3))
! component parallel to vertical on surface p
          a(1)=intersect(1)-xc(p,1)
          a(2)=intersect(2)-xc(p,2)
          a(3)=intersect(3)-xc(p,3)
          b(1)=vert(p,1)
          b(2)=vert(p,2)
          b(3)=vert(p,3)
          vcomp=dabs(a(1)*b(1)+a(2)*b(2)+a(3)*b(3))
          if ((hcomp <= (w(p)/2.d0)).and.(vcomp <= (h(p)/2.d0))) then
            shadow=.true.
!          write(6,*) 'shadow'
          else
!          write(6,*) 'no shadow'
          end if
          end if
!          stop
! check for interference of reflected ray with surface 1 (absorber)
          p=1
          if (.not.shadow) then
! calculate distance from source to center of p
          dist(1)=origin(1)-xc(p,1)
          dist(2)=origin(2)-xc(p,2)
          dist(3)=origin(3)-xc(p,3)
```

```
        scale=(dist(1)*normal(p,1)+dist(2)*normal(p,2)+
     >          dist(3)*normal(p,3))/
     >        (reflecdir(1)*normal(p,1)+reflecdir(2)*normal(p,2)+
     >          reflecdir(3)*normal(p,3))
        dot=-(reflecdir(1)*normal(p,1)+reflecdir(2)*normal(p,2)
     >        +reflecdir(3)*normal(p,3))
!         power2=power1*dot
        power2=power1*abs(dot)/dot ! don't need the dot product, power is the same whichever way it hits the surface
!        write(6,*) 'scale=',scale,power2
!        write(6,*) origin
!        write(6,*) origin-incoming
!        write(6,*) origin
!        write(6,*) origin+reflecdir
!        stop
! point of intersection
        intersect(1)=origin(1)-scale*reflecdir(1)
        intersect(2)=origin(2)-scale*reflecdir(2)
        intersect(3)=origin(3)-scale*reflecdir(3)
! component parallel to horizontal on surface p
        a(1)=intersect(1)-xc(p,1)
        a(2)=intersect(2)-xc(p,2)
        a(3)=intersect(3)-xc(p,3)
        b(1)=horiz(p,1)
        b(2)=horiz(p,2)
        b(3)=horiz(p,3)
        hcomp=dabs(a(1)*b(1)+a(2)*b(2)+a(3)*b(3))
! component parallel to vertical on surface p
        a(1)=intersect(1)-xc(p,1)
        a(2)=intersect(2)-xc(p,2)
        a(3)=intersect(3)-xc(p,3)
        b(1)=vert(p,1)
        b(2)=vert(p,2)
        b(3)=vert(p,3)
        vcomp=dabs(a(1)*b(1)+a(2)*b(2)+a(3)*b(3))
        if ((hcomp <= (w(p)/2.d0)).and.(vcomp <= (h(p)/2.d0))) then
! uncomment line below to print out intersection point
!          write(6,*) intersect
          if (power2 >= 0.d0) then
           heat_rate_out=heat_rate_out+power2
          end if
!          write(6,*) 'intersect',heat_rate_out,power2
        else
!          write(6,*) 'no intersect'
        end if
!        stop
       end if
      end do
     end do
    end do
!
    return
    end
!
!-----------------------------------------------------------------------
!
    subroutine sun_direction1(t_in,dir)
!
    implicit none
```

```
      integer t_in,time
      double precision,dimension(3) :: dir
      double precision :: mag
!
      time=t_in
!      write(6,*) 'time',time
      dir(1)=0.8
      dir(2)=-0.4
      dir(3)=-0.3
      mag=dsqrt(dir(1)**2+dir(2)**2+dir(3)**2)
      dir=dir/mag

      return
      end
!
!----------------------------------------------------------------------
!
      subroutine surf_pre_proc
!
      use surf_data
      implicit none
!
      ! read surface file header
      open(unit=11,form='formatted',file='surf_def.txt')
      read(11,*) nsurf,nx,ny,ncase
      allocate(xc(nsurf,3))
      allocate(normal(nsurf,3))
      allocate(horiz(nsurf,3))
      allocate(vert(nsurf,3))
      allocate(w(nsurf))
      allocate(h(nsurf))
!
      return
      end
!
!----------------------------------------------------------------------
!
      subroutine surf_proc
!
      use surf_data
      implicit none
      integer i,j,n,m
      double precision,dimension(3) :: a,b,c,corner
      double precision mag
!
      ! read surface parameters
      do i=1,nsurf
       read(11,*) (xc(i,j),j=1,3),(normal(i,j),j=1,3),w(i),h(i)
      end do
!      close(11)
!
! for each surface, set up local coordinate system
      do i=1,nsurf
       mag=dsqrt(normal(i,1)**2+normal(i,2)**2+normal(i,3)**2)
       normal(i,1)=normal(i,1)/mag
       normal(i,2)=normal(i,2)/mag
       normal(i,3)=normal(i,3)/mag ! normalized z axis
!
```

```
      horiz(i,1)=-normal(i,2)
      horiz(i,2)=normal(i,1)
      horiz(i,3)=0.d0
      mag=dsqrt(horiz(i,1)**2+horiz(i,2)**2+horiz(i,3)**2)
      horiz(i,1)=horiz(i,1)/mag
      horiz(i,2)=horiz(i,2)/mag
      horiz(i,3)=horiz(i,3)/mag ! normalized horizontal axis
!
      a(1)=normal(i,1)
      a(2)=normal(i,2)
      a(3)=normal(i,3)
      b(1)=horiz(i,1)
      b(2)=horiz(i,2)
      b(3)=horiz(i,3)
      call cross(a,b,c)
!      write(6,*) a,b,c
      vert(i,1)=c(1)
      vert(i,2)=c(2)
      vert(i,3)=c(3)
      end do
!
! output surface vertices
! uncomment write lines below to output vertices
      do i=1,nsurf
      corner(1)=xc(i,1)-w(i)*horiz(i,1)/2.d0-h(i)*vert(i,1)/2.d0
      corner(2)=xc(i,2)-w(i)*horiz(i,2)/2.d0-h(i)*vert(i,2)/2.d0
      corner(3)=xc(i,3)-w(i)*horiz(i,3)/2.d0-h(i)*vert(i,3)/2.d0
!      write(6,*) (corner(j),j=1,3)
      corner(1)=xc(i,1)+w(i)*horiz(i,1)/2.d0-h(i)*vert(i,1)/2.d0
      corner(2)=xc(i,2)+w(i)*horiz(i,2)/2.d0-h(i)*vert(i,2)/2.d0
      corner(3)=xc(i,3)+w(i)*horiz(i,3)/2.d0-h(i)*vert(i,3)/2.d0
!      write(6,*) (corner(j),j=1,3)
      corner(1)=xc(i,1)+w(i)*horiz(i,1)/2.d0+h(i)*vert(i,1)/2.d0
      corner(2)=xc(i,2)+w(i)*horiz(i,2)/2.d0+h(i)*vert(i,2)/2.d0
      corner(3)=xc(i,3)+w(i)*horiz(i,3)/2.d0+h(i)*vert(i,3)/2.d0
!      write(6,*) (corner(j),j=1,3)
      corner(1)=xc(i,1)-w(i)*horiz(i,1)/2.d0+h(i)*vert(i,1)/2.d0
      corner(2)=xc(i,2)-w(i)*horiz(i,2)/2.d0+h(i)*vert(i,2)/2.d0
      corner(3)=xc(i,3)-w(i)*horiz(i,3)/2.d0+h(i)*vert(i,3)/2.d0
!      write(6,*) (corner(j),j=1,3)
      end do
!      write(6,*) 'vertices end here'
!
! put grid on surfaces 2+
      allocate(xs(nsurf,nx+1,ny+1,3))
      do i=2,nsurf
      do n=1,nx+1
       do m=1,ny+1
       xs(i,n,m,1)=xc(i,1)-w(i)*horiz(i,1)/2.d0-h(i)*vert(i,1)/2.d0
     >             +w(i)*horiz(i,1)/nx*(n-1)+h(i)*vert(i,1)/ny*(m-1)
       xs(i,n,m,2)=xc(i,2)-w(i)*horiz(i,2)/2.d0-h(i)*vert(i,2)/2.d0
     >             +w(i)*horiz(i,2)/nx*(n-1)+h(i)*vert(i,2)/ny*(m-1)
       xs(i,n,m,3)=xc(i,3)-w(i)*horiz(i,3)/2.d0-h(i)*vert(i,3)/2.d0
     >             +w(i)*horiz(i,3)/nx*(n-1)+h(i)*vert(i,3)/ny*(m-1)
!      write(6,*) (xs(i,n,m,j),j=1,3)
       end do
      end do
      end do
```

Appendix A. Simulation FORTRAN code

```
!
      return
      end
!
!----------------------------------------------------------------------
!
      subroutine cross(a,b,c)
!
      implicit none
      double precision,dimension(3) :: a,b,c
!
      c(1)=a(2)*b(3)-a(3)*b(2)
      c(2)=a(3)*b(1)-a(1)*b(3)
      c(3)=a(1)*b(2)-a(2)*b(1)
!
      return
      end
!
!----------------------------------------------------------------------
!
      subroutine sun_direction(time_in,direction)
!
      implicit none
      integer day
      double precision,dimension(3) :: direction
      double precision :: time_in
      double precision :: delta
      double precision :: c1
      double precision :: c2
      double precision :: c3
      double precision :: gamap
      double precision :: gamas
      double precision :: pi
      double precision :: wew
      double precision :: thetaz
      double precision :: phi
      double precision :: omega
!
! calculations based on duffie and beckman p. 13+
!
      pi=4.d0*datan(1.d0)
      phi=35.08/180.d0*pi ! latitude for Albuquerque NM!!!
! day angle
      day=int(time_in/(24*3600))+1
! declination
      delta=(23.45*dsin(2.d0*pi*(284.d0+day)/365.25d0))/180.d0*pi
! hour angle
      omega=(time_in-(day-1)*86400.d0-43200.d0)/43200.d0*pi
! zenith angle
      thetaz=dacos(dcos(phi)*dcos(delta)*dcos(omega)
     >       +dsin(phi)*dsin(delta))
! azimuth angle
      wew=dacos(dtan(delta)/dtan(phi))
      if (dabs(omega) < wew) then
       c1=1.d0
      else
       c1=-1.d0
      end if
```

```
      if ((phi*(phi-delta)) >= 0.d0) then
       c2=1.d0
      else
       c2=-1.d0
      end if
      if (omega >= 0.d0) then
       c3=1.d0
      else
       c3=-1.d0
      end if
      gamap=dasin(dsin(omega)*dcos(delta)/dsin(thetaz))
      gamas=c1*c2*gamap+c3*((1.d0-c1*c2)/2.d0)*pi
!
!      write(6,*) time_in,thetaz,gamas
!     write(6,*) 'time',time_in
!     write(6,*) 'delta',delta
!     write(6,*) 'day',day
!     write(6,*) 'hour',omega
!     write(6,*) 'zenith',thetaz
!     write(6,*) 'azimuth',gamas
!     stop
!
      direction(1)=-dcos(-gamas)*dsin(thetaz)
      direction(2)=-dsin(-gamas)*dsin(thetaz)
      direction(3)=-dcos(thetaz)
!     write(6,*) time_in,direction
!
      return
      end
```

References

[1] Yazaki. Yazaki solar air conditioning absorption chiller wfc-s series 10, 20, and 30 rt cooling. `www.solarpanelsplus.com/yazaki-solar-HVAC/`.

[2] M. L. Ortiz. A trnsys model of a solar thermal system with thermal storage and absorption cooling. Master's thesis, University of New Mexico, December 2008.

[3] Ltd. Beijing Sunda Solar Energy Technology Co. Seido technology. Internet. `www.sundasolar.com/product_technology.html`.

[4] Ltd. Beijing Sunda Solar Energy Technology Co. Seid01 series heat pipe vacuum tube solar collector. Internet. `www.sundasolar.com/product_index.html`.

[5] Reflectech, Inc., 18200 West Highway 72, Arvada, CO, 80007. *Reflectech Mirror Film*.

[6] G. J. Jorgensen and R. Gee. Durable corrosion and ultraviolet-resistant silver mirror, 2006.

[7] M. DiGrazia, R. Gee, and G. Jorensen. Reflectech mirror film attributes and durability for csp applications. In *Proceedings of ES2009, Energy Sustainability 2009*, July 2009.

[8] J. A. Duffie and W. A. Beckman. *Solar Engineering of Thermal Processes*. John Wiley & Sons, Inc., second edition, 1991.

REFERENCES

[9] C. S. Park. *Contemporary Engineering Economics*. Addison-Wesley, second edition, 1997.

[10] Albuquerque weather data. `www.nmts.org/albuquerque_weather_data.htm`.

[11] M. W. Wildin. Results from use of thermally stratified water tanks to heat and cool the mechanical engineering building at the university of new mexico. Technical report, Oak Ridge National Laboratory, June 1983.

[12] U.S. Energy Information Administration Independent Statistics and Analysis. Wellhead acquisition price by first purchasers (dollars per barrel), August 2010. `http://www.eia.doe.gov/dnav/pet/hist/LeafHandler.ashx?n=pet&s=f000000__3&f=a`.

[13] H. Tabor. Stationary mirror systems for solar collectors. *Solar Energy*, 2:27–33, 1958.

[14] H. Tabor. Mirror boosters for solar collectors. *Solar Energy*, 10(3):111–118, 1966.

[15] A.F. Souka and H.H. Safwat. Optimum orientations for the double-exposure, flat-plate collector and its reflectors. *Solar Energy*, 10(4):170–174, 1966.

[16] D.L. Merchant and H.H Cobble. Mirror solar panels. *Solar Energy*, 10(3):150–152, 1966.

[17] A.F. Souka and H.H. Safwat. Theoretical evaluation of the perfromance of a double exposure flat-plate collector using a single reflector. *Solar Energy*, 12(3-E):347–352, 1969.

[18] H.E. Thomason and H.J.L. Thomason Jr. Solar housese/heating and cooling progress report. *Solar Energy*, 15(1-C):27–39, 1973.

REFERENCES

[19] D.K. McDaniels, D.H. Lowndes, H. Mathew, J. Reynolds, and R. Gray. Enhanced solar energy collection using reflector-solar thermal collector combinations. *Solar Energy*, 17(5-B):277–283, 1975.

[20] S.C. Seitel. Collector performance enhancement with flat reflectors. *Solar Energy*, 17(5-D):291–295, 1975.

[21] S.L. Grassie and N. R. Sheridan. The use of planar reflectors for increasing the energy yield of flat-plate collectors. *Solar Energy*, 19(6-F):663–668, 1977.

[22] S. Baker, D.K. McDaniels, H.D. Kaehn, and D.H. Lowndes. Technical note: Time integrated calculation of the insolation collected by a reflector. *Solar Energy*, 20:415–417, 1978.

[23] P.N. Espy. Solar thermal collectors using planar reflector. *International Solar Energy Society*, 2:1038–1042, 1978.

[24] D. P. Grimmer, K.G. Zinn, K.C. Herr, and B.E. Wood. Augmented solar energy collection using various planar reflective surfaces: Theoretical calculations and experimental results. *Los Alamos Scientific Laboratory of the University of California*, LA-7041, April 1978.

[25] K.D. Mannan and R.B. Bannerot. Optimal geometries for one- andtwo-faced symmetric side-wall booster mirrors. *Solar Energy*, 21(5-C):385–391, 1978.

[26] R.B. Bannerot and J.R. Howell. Predicted daily and yearly average radiative performance of optimal trapezoidal groove solar energy collector. *Solar Energy*, 22:229–234, 1979.

[27] D.C. Larson. Mirror enclosures for double-exposure solar collectors. *Solar Energy*, 23(6-E):517–524, 1979.

[28] D.C. Larson. Technical note: Optimization of flat-plate collector-flat mirror systems. *Solar Energy*, 24(2-G):203–207, 1980.

REFERENCES

[29] F.A. Rudloff, S.R. Swanson, and R.F. Boehm. Computer simulation results for planar reflectors and flat plate solar collectors. *Journal of Solar Energy Engineering*, 102:166–172, May 1980.

[30] I.S. Taha and S.M. Eldighidy. Effect of off-south orientation on optimum conditions for maximum solar energy absorbed by flat plate collector augmented by plane reflector. *Solar Energy*, 25:373–379, 1980.

[31] H.F. Chiam. Planar concentrators for flat-plate solar collectors. *Solar Energy*, 26:503–509, 1981.

[32] H.F. Chiam. Stationary reflector-augmented flat-plate collectors. *Solar Energy*, 29:65–69, 1982.

[33] H.F. Chiam. Bi-yearly adjusted v-trough concentrators. *Solar Energy*, 28:407–412, 1982.

[34] H.F. Chiam. Planar solar reflectors. *International Journal of Ambient Energy*, 3(4):195–202, October 1982.

[35] H.P. Garg and D.S. Hrishikesan. Enhancement of solar energy on flat-plate collector by plane booster mirrors. *Solar Energy*, 40:295–307, 1988.

[36] D. Faiman and A. Zemel. Low-profile solar water heaters: The mirror booster problem revisited. *Solar Energy*, 40(4):385–390, 1988.

[37] S.C. Kaushik, R. Kumar, S.Chandra, and S.Kaul. Solar collector-reflector systems; state of art study and performance evaluation. *International Journal of Sustainable Energy*, 16:245–262, 1995.

[38] H.M.S. Hussein, G.E. Ahmad, and M.A. Mohamad. Optimization of operational and design parameters of plane reflector-tilted flat plate solar collector systems. *Energy*, 25(6):529–542, June 2000.

REFERENCES

[39] R. Siegel and J. R. Howell. *Thermal Radiation Heat Transfer*. Taylor & Francis, fourth edition, 2002.

[40] W. Rasband. Imagej 1.41o. `rab.info.nih.gov/ij`.

[41] Inc. ReflecTech, 2010. `www.reflectechsolar.com/pricing.html`.

[42] Salary.com. Salary.com, October 2010. `www.salary.com`.

[43] E. P. DeGarmo, J T. Black, and R. A. Kohser. *Materials and Processes in Manufacturing*. Prentice Hall, eigth edition, 1997.

[44] K. Hitomi. *Manufacturing Systems Engineering*. Taylor & Francis, 1996.

[45] G. T. Ortiz. Public service company of new mexico electric services, 2010. `www.pnm.com/regulatory/pdf_electricity/schedule_3_b.pdf`.

[46] Tucson Electric Power. Time-of-use-rates, 2010. `www.tucsonelectric.com/Home/Programs/PricingPlans/PricingPlanSummary.asp`.

[47] Pacific Gas & Electric. Commercial current, 2006. `www.pge.com/tariffs/CommercialCurrent.xls`.